REDEMAT

REDE TEMÁTICA EM ENGENHARIA DE MATERIAIS

UFOP – CETEC – UEMG

Tese de Doutorado

CINÉTICA DE LIXIVIAÇÃO DOS CONCENTRADOS DE ZINCO UTILIZADOS NA VOTORANTIM METAIS

Autor: Adelson Dias de Souza
Orientador: Professor Versiane Albis Leão (DSc)
Co-orientador: Professor Carlos Antônio da Silva (PhD)

Ouro Preto, Novembro de 2007

REDEMAT

UFOP – CETEC - UEMG

Adelson Dias de Souza

"CINÉTICA DE LIXIVIAÇÃO DOS CONCENTRADOS DE ZINCO UTILIZADOS NA VOTORANTIM METAIS"

Tese de Doutorado apresentada ao Programa de Pós-Graduação em Engenharia de Materiais da REDEMAT, como parte integrante dos requisitos para a obtenção do título de Doutor em Engenharia de Materiais.

Área de concentração: Processos de fabricação

Orientador: Professor Versiane Albis Leão (DSc)

Co-orientador: Professor Carlos Antônio da Silva (PhD).

Ouro Preto, novembro de 2007

S729c **Souza, Adelson Dias de.**

Cinética de lixiviação dos concentrados de zinco utilizados na Votorantin Metais [manuscrito] / Adelson Dias de Souza. – 2007.
xiv, 98f. : il.; graf., tabs.

Orientador: Prof. Dr. Versiane Albis Leão.
Co-orientador: Prof. Dr. Carlos Antônio da Silva.

Tese (Doutorado) - Universidade Federal de Ouro Preto. Rede Temática em Engenharia de Materiais.

Área de concentração: Processos de fabricação.

1. Lixiviação química - Teses. 2. Zinco - Teses. 3. Silicatos - Teses. 4. Sulfetos - Teses. I. Universidade Federal de Ouro Preto. II. Título.

CDU: 669.5

Catalogação: sisbin@sisbin.ufop.br

A meus pais, Maria do Carmo Souza e Sidney Teixeira de Souza, que, se estivessem vivos, estariam com certeza expressando o orgulho deste momento.

À minha esposa Cristina e meus filhos Felipe e Tasso, que souberam entender as ausências, justificadas pelo desenvolvimento deste trabalho.

"A melhor maneira de predizer o futuro é inventá-lo."

Alan Kay

AGRADECIMENTOS

Primeiramente, ao Prof. Dr. Versiane Albis Leão, por sua dedicação profissional, por sempre estar disponível a dar a orientação necessária para a realização dos trabalhos, tanto práticos, como de discussão de propostas, modelos, resultados e, por fim, da elaboração final da tese. Mais do que todo esse suporte técnico, vale ressaltar sua capacidade de motivar e de coordenar, para que os objetivos fossem atingidos.

Ao co-orientador Prof. Dr. Carlos Silva, por sua experiência e por orientar quanto aos caminhos a serem percorridos nos momentos de indecisão ou de maior complexidade.

À Votorantim Metais Zinco (VMZ), que contribuiu em todos os sentidos para que o doutorado fosse desenvolvido, desde a apresentação inicial por nosso Superintendente João Bosco Silva. A VMZ sustentou com recursos as iniciativas práticas e me proporcionou, através de bolsa de seu programa de formação de "experts", toda a realização deste trabalho.

À UFOP e à REDEMAT, pelo conhecimento proporcionado através de seus competentes professores.

Ao colega de mestrado e doutorado, Pablo Pina, por poder contar sempre com seu suporte, discutindo propostas, ajudando no direcionamento dos experimentos e participando como co-autor dos artigos publicados.

Por fim, ao José Antônio de Magalhães, de Votorantim Metais Zinco Três Marias, companheiro imprescindível desde o mestrado, por sua colaboração durante os experimentos e na discussão dos resultados.

RESUMO

A cinética de lixiviação de concentrados de zinco (sulfetados e silicatados) foi estudada no presente trabalho. Primeramente, foram avaliados os efeitos de temperatura, concentrações de íon férrico e ácido sulfúrico, velocidade de agitação e tamanho de partícula sobre a cinética de lixiviação de um concentrado sulfetado em soluções ácidas de sulfato férrico. O processo de lixiviação pôde ser separado em dois estágios. Inicialmente, a cinética de dissolução do concentrado sulfetado era controlada por reação química na superfície das partículas de sulfeto de zinco. Posteriormente, a cinética de dissolução era controlada pela difusão do íon férrico através da camada de enxofre elementar (camada de cinza) formada na superfície do sólido. A energia de ativação da etapa controlada por reação química foi de 6,6kcal/mol (27,5kJ/mol) e o valor encontrado para o estágio final, controlado por difusão do reagente na camada de produto foi de 4,7kcal/mol (19,6kJ/mol). As ordens de reação com respeito à concentração de íon férrico e ácido sulfúrico eram cerca de 0,50 e 1,00, respectivamente. As análises de MEV-EDS das partículas de sulfeto "in natura" e lixiviadas mostraram um progressivo aumento da espessura da camada de enxofre elementar sobre a superfície do sólido. A formação desta camada de enxofre era uma evidência adicional da mudança da etapa controladora do processo de dissolução do sulfeto com o progresso da reação. Também foi estudada a cinética de lixiviação do concentrado calcinado de silicato de zinco, incluindo os efeitos do tamanho de partícula (0,038–0,075mm), temperatura (30^{o}C–50^{o}C) e concentração inicial de ácido (0,2–1,0 mol/L). Os resultados mostraram que a redução do tamanho de partícula aumenta levemente a velocidade de lixiviação, enquanto a temperatura e a concentração de ácido sulfúrico têm uma grande influência na dissolução. À medida que ocorre a lixiviação, há uma progressiva dissolução da willemita mantendo-se as fases ricas em quartzo e ferro praticamente inertes. Dentre os modelos cinéticos aplicados a sólidos porosos testados no presente trabalho, o "modelo do grão" com controle por difusão nos poros descreveu de forma satisfatória a cinética de dissolução do concentrado calcinado silicatado de zinco. Através da utilização deste modelo, foi possível determinar a energia de ativação e ordem de reação com respeito a concentração de ácido sulfúrico, obtendo os valores de 50,7kJ/mol e 0,64, respectivamente, os quais são, provavelmente, conseqüências da natureza paralela dos processos de difusão e reação química no sólido poroso. Além disto, os estudos de lixiviação do silicato de zinco mostraram que o teor de ferro no concentrado silicatado de zinco não afeta a extração de zinco, uma vez que a cinética de dissolução dos concentrados com alto teor (10-11%) ou baixo teor (3%) é similar. A energia de ativação encontrada para a lixiviação do concentrado de alto ferro, 13,1±5,1kcal/mol, era estatisticamente igual àquela observada para o material com baixo teor de ferro, 16,0±2,2kcal/mol, sugerindo que o processo de dissolução de ambos os materiais seja controlado pela mesma etapa controladora. As análises estatísticas dos experimentos de lixiviação mostraram que o aumento do teor de ferro no silicato de 5% para 9% não resultou em redução significativa nas extrações. Para os concentrados de baixo teor, a extração foi de 98,5% enquanto que para os de alto teor foi de 97,5%. Além disto, o concentrado com alto teor de ferro viabiliza uma maior recuperação de massa durante o processo de flotação do minério silicatado. Foi proposta uma nova rota tecnológica para utilização de concentrado com alto teor de ferro, que inclui a remoção de impurezas (Ge, As, Sb), eliminando a necessidade de integração com processo RLE.

ABSTRACT

The leaching kinetics of zinc concentrates (suphides and silicates) was studied. Firstly, the effects of temperature, ferric ion and sulphuric acid concentrations, agitation speed and particle size on the leaching kinetics of a zinc sulphide concentrate in acid ferric sulphate medium were investigated. The leaching process could be separated into two stages. Initially, the dissolution kinetics was controlled by the chemical reaction at the surface of the zinc sulphide particles followed by a second step where the reaction was controlled by diffusion of the reagents or products through the elemental sulphur (ash) layer. The activation energy of the chemical controlled step was 6.6kcal/mol (27.5kJ/mol) and the value determined for the diffusion controlled step was 4.7kcal/mol (19.6kJ/mol). The reaction order with respect to ferric ion and sulphuric acid concentrations were approximately 0.50 and 1.00, respectively. Analysis of the unreacted and reacted sulphide particles by SEM-EDS showed a progressive increase of the thickness of the elemental sulphur layer on the solid surface. The development of this sulphur layer was a further evidence of the change on the rate-controlling step as the reaction progress. Also studied was the leaching kinetics of the zinc silicate calcine including the effects of particle size (0.038–0.075mm), temperature (30^{o}C–50^{o}C) and initial acid concentration (0.2–1.0 mol/L). The results showed that decreasing particle size slightly increases the leaching rate, while temperature and acid concentration have a stronger effect on dissolution. As leaching occurs, there is a progressive dissolution of willemite while the quartz and iron-containing phases remain inert. Among the kinetic models for porous solids tested, the grain model with porous diffusion control successfully described the zinc dissolution kinetics. The model enabled the determination of an activation energy and reaction order with respect to sulphuric acid values of 50.7kJ/mol and 0.64, respectively, which are likely a consequence of the parallel nature of diffusion and chemical reaction in porous solids. In addition, zinc silicate leaching studies have shown that the iron content in zinc silicate concentrates does not affect zinc extraction as the dissolution kinetics of concentrates with either high (10-11%) or low iron (3%) content are similar. The activation energy determined for the high-iron concentrate leaching, 13.1±5.1kcal/mol, was statistically similar to that observed for the low-iron material, 16.0±2.2kcal/mol. This suggests that the leaching of both solids presents the same rate-controlling step. The statistical analysis of the leaching experiments showed that increasing the iron content of the silicate from 5% to 9% iron does not result in a significant reduction in extractions, as 98.5% zinc dissolution was achieved for the low-iron concentrate. In the meantime, a zinc extraction of 97.5% was observed for the high-iron sample. Furthermore, high iron contents in the silicate concentrate enable a higher mass recovery during flotation. A flowsheet was proposed utilizing the high iron content of the silicate to remove impurities during the hydrometallurgical processing of zinc silicates.

SUMÁRIO

LISTA DE FIGURAS

LISTA DE TABELAS

CAPÍTULO 1

1. INTRODUÇÃO

1.1. Lixiviação de concentrados sulfetados de zinco

Atualmente, mais de 80% da produção mundial de zinco é proveniente do tratamento de concentrado sulfetado, onde a esfalerita $(Zn_2Fe)S_2$ é o mineral predominante (Dutrizac, 2005). O processo hidrometalúrgico tradicional de tratamento de concentrados sulfetados de zinco compreende a ustulação, lixiviação e eletrólise (Feneau, 2002), denominado RLE ("Roasting, Leaching and Electrolysis"). Basicamente, este processo inclui a ustulação dos sulfetos de zinco, produzindo óxidos dos metais e dióxido de enxofre. Este último é convertido em ácido sulfúrico (H_2SO_4). A reação química da etapa de ustulação é a seguinte:

$$ZnS(s) + 1{,}5O_2(g) \rightarrow ZnO(s) + SO_2(g) \qquad (1.1)$$

O calcinado (ZnO) produzido de acordo com a equação 1.1 é enviado para etapas de lixiviação, seguido de purificação, eletrólise e fusão, produzindo o zinco SHG ("special high grade"), de alta pureza, com no mínimo 99,995% em zinco. As reações principais das etapas de lixiviação neutra (1.2) e ácida (1.3) são (Feneau, 2002):

$$ZnO(s) + 2H_2SO_4(aq) \rightarrow ZnSO_4(aq) + H_2O(aq) \qquad (1.2)$$

$$ZnO.Fe_2O_3(s) + 4H_2SO_4(aq) \rightarrow Fe_2(SO_4)_3(aq) + ZnSO_4(aq) + 4H_2O(aq) \qquad (1.3)$$

Contudo, a rota RLE tem algumas restrições ao tratamento dos concentrados de zinco, especialmente aqueles com elevados teores de sílica, cálcio, cobre e ferro. Também a emissão de SO_2 deste processo e o mercado de ácido sulfúrico são desafios para o futuro desta tecnologia (Feneau, 2002).

Devido a estas restrições e à dependência do processo RLE com relação à produção de ácido sulfúrico, vem havendo um crescente interesse nas técnicas de lixiviação direta de concentrados sulfetados de zinco. Na lixiviação direta, o íon sulfeto não se converte em ácido, mas em enxofre elementar, de fácil estocagem. Como alternativa, duas rotas similares foram propostas nos anos 70: (i) *Lixiviação Direta Amosférica* (Svens et al., 2003) na qual os concentrados sulfetados de zinco são lixiviados diretamente com solução de ferro férrico, produzida durante as etapas de lixiviação ácidas do processo RLE; e (ii) *Lixiviação Direta Sob Pressão*, que adota um conceito similar, exceto que a lixiviação é conduzida em autoclaves (14-15 atm).

As reações de lixiviação direta dos concentrados sulfetados de zinco ainda não estão totalmente compreendidas, embora haja um acordo generalizado de que a reação do sulfato férrico com a esfalerita tem um papel importante no processo de dissolução de zinco (Dutrizac, 2005). Neste caso, a lixiviação direta do ZnS pelo Fe(III) pode ser representada pela equação 1.4:

$$Fe_2(SO_4)_3(aq) + ZnS(s) \rightarrow 2FeSO_4(aq) + ZnSO_4(aq) + S°(s) \qquad (1.4)$$

Oxigênio gasoso (93-98%) é geralmente usado para reoxidar o ferro ferroso, obtido através da equação 1.4, regenerando o Fe(III), segundo equação 1.5.

$$2\ FeSO_4(aq) + H_2SO_4(aq) + 0.5O_2(g) \rightarrow Fe_2(SO_4)_3(aq) + H_2O(l) \quad (1.5)$$

A reação global de lixiviação pode ser representada pela equação 1.6.

$$ZnS(s) + H_2SO_4(aq) + 0.5O_2(g) \rightarrow ZnSO_4(aq) + H_2O(l) + S°(s) \quad (1.6)$$

A elevada pressão de oxigênio, verificada no processo de lixiviação sob pressão proporciona um menor tempo de residência, da ordem de 90 minutos. De modo contrário, o processo de lixiviação direta atmosférica requer cerca de 24 horas para que a reação se complete. Desta forma, os reatores de lixiviação direta atmosférica são muito maiores quando comparados com o tamanho de autoclaves do processo de lixiviação sob pressão (Svens et al., 2003).

O emprego da tecnologia de lixiviação sob pressão teve início em escala industrial no ano de 1981, na unidade de Cominco Trail, em Trail, British Columbia, no Canadá, onde se integrou com o sistema existente de ustulação-lixiviação-eletrólise RLE (Svens et al., 2003). A mesma tecnologia, porém sem integração com o processo RLE, está também em operação na unidade industrial de Flin Flon, em "Hudson Bay", desde 1993. Uma outra usina de lixiviação sob pressão foi instalada no Cazaquistão, em 2003 (Svens et al., 2003).

Já a lixiviação direta atmosférica foi implementada em 1994, na unidade industrial da "Onsan Korea Zinc", na Coréia do Sul. Em 1998, o processo foi implantado na unidade industrial de Kokkola, na Finlândia e, mais recentemente, na unidade industrial de

"Odda Zinc", na Noruega, sendo que no total já se produz mais de 200 mil toneladas de zinco por ano por esta tecnologia. (Svens et al., 2003).

Ambos os processos de lixiviação direta atmosférica e sob pressão, são considerados marcos na indústria global do zinco. Além disto, o custo de capital "capex" ("capital expenditure") são mais baixos para se implantar a lixiviação direta de concentrados sulfetados de zinco. Entretanto, o custo operacional "opex" ("operating and maintenance costs") tem sido considerado relativamente elevado devido principalmente ao grande consumo de oxigênio, matéria-prima relativamente cara (Souza et al., 2007).

A fim de reduzir o "opex", uma combinação entre biolixiviação e lixiviação química direta de concentrados sulfetados de zinco foi proposta por Souza et al. (2007), como um processo de custo mais competitivo do que as tecnologias de lixiviação direta atmosférica ou sob pressão. A biolixiviação parcial do concentrado sulfetado de zinco num processo contínuo, com microrganismo mesófilo, capaz de oxidar o íon ferroso, foi estudada pelos autores. Os resultados demonstraram ser possível projetar uma nova tecnologia capaz de obter até 96% de recuperação de zinco, extração similar ao processo convencional RLE.

Em termos de lixiviação direta, é raro encontrar artigos publicados com estudos para os concentrados sulfetados de zinco da América do Sul. A cinética de lixiviação por íon férrico para outras fontes de sulfetos de zinco tem sido descrita por diversos autores (Dutrizac, 1992; Dutrizac, 2005; Markus et al., 2004; Perez and Dutrizac, 1991). É consenso que o enxofre elementar é o principal produto de oxidação e o ferro contido na esfalerita tem um papel chave durante a lixiviação. Foi observado que a temperatura

aumenta a velocidade de reação, mas os valores de energia de ativação registrados variam amplamente (Perez and Dutrizac, 1991). Ademais, apesar do efeito da concentração de ácido na dissolução do zinco estar bem caracterizado, a ordem de reação com respeito à concentração de ácido sulfúrico foi pouca estudada (Crundwell, 1988).

1.2 Lixiviação dos concentrados de silicato de zinco

Sabe-se que mesmo antes do século 20, os minérios não-sulfetados já eram importante fontes de zinco no mundo, sendo constituídos de uma mistura de silicatos, carbonatos e óxidos, especialmente calamina. Zinco era produzido em minas espalhadas na Europa e utilizado para produzir latão, ligas de zinco-cobre-estanho. As tecnologias recentes para tratar os silicatos de zinco, como o "Processo integrado de tratamento de concentrados de silicato e sulfetos de zinco", em operação na unidade industrial de Três Marias, no Brasil, e MZP ("Modified Zincex Process") que utiliza extração por solventes e implantado na unidade industrial de "Skorpion Zinc", na Namíbia, têm proporcionado renovado interesse comercial nestes materiais. O foco econômico é indubitável para os depósitos de zinco oxidados, devido às muitas vantagens sobre os depósitos de sulfetos (Boni, 2005):

- Alto teor de zinco se comparado com os sulfetos (zinco > 10%).
- Em geral, pode ser explorado em mineração a céu aberto.
- Devido à baixa dureza, necessitariam pequenas perfuratrizes/explosões.
- Possuem forma natural de "cut off".

Em breve, a produção anual de zinco através de fontes de não-sulfetados deve exceder a 10% da produção mundial do metal (Boni, 2005). As minas de Vazante, no Brasil, estão produzindo 150 mil toneladas de zinco em 2007 e projetam extrair 200 mil toneladas do metal contido já em 2010, a partir de silicatos de zinco, cujo concentrado é enviado para a unidade industrial de Três Marias. Também a "Skorpion Zinc", na Namíbia, está produzindo atualmente mais de 160 mil toneladas de zinco a partir de silicatos e carbonatos, para alimentar seu processo de extração por solventes. Somente as contribuições destas duas indústrias já representam mais de 3% da produção global do metal.

Os concentrados não-sulfetados são difíceis de serem tratados, devido aos elevados níveis de sílica, germânio e antimônio contidos e os custos de seu processamento podem ser elevados, por não gerarem créditos de ácido sulfúrico, como no tratamento dos concentrados sulfetados. A alternativa encontrada pela Votorantim Brasil, na década de 90, para solucionar tais problemas, foi usar as vantagens da integração com o tratamento de concentrados sulfetados, devido à geração de ácido sulfúrico e o elevado poder purificante do calcinado (ZnO), na etapa de Lixiviação Neutra. O fluxograma da integração em uma das possíveis rotas é mostrado na figura 1.1.

Usando também minerais não-sulfetados, como carbonatos e silicatos, a empresa Técnicas Reunidas (TR), da Espanha, desenvolveu o Processo Zincex Modificado, chamado de MZP, e implantou a técnica na unidade de "Skorpion Zinc", em 2003. O processo usa um solvente orgânico (DEHPA, dissolvido em querosene), sendo que o fluxograma resumido do processo é mostrado na figura 1.2.

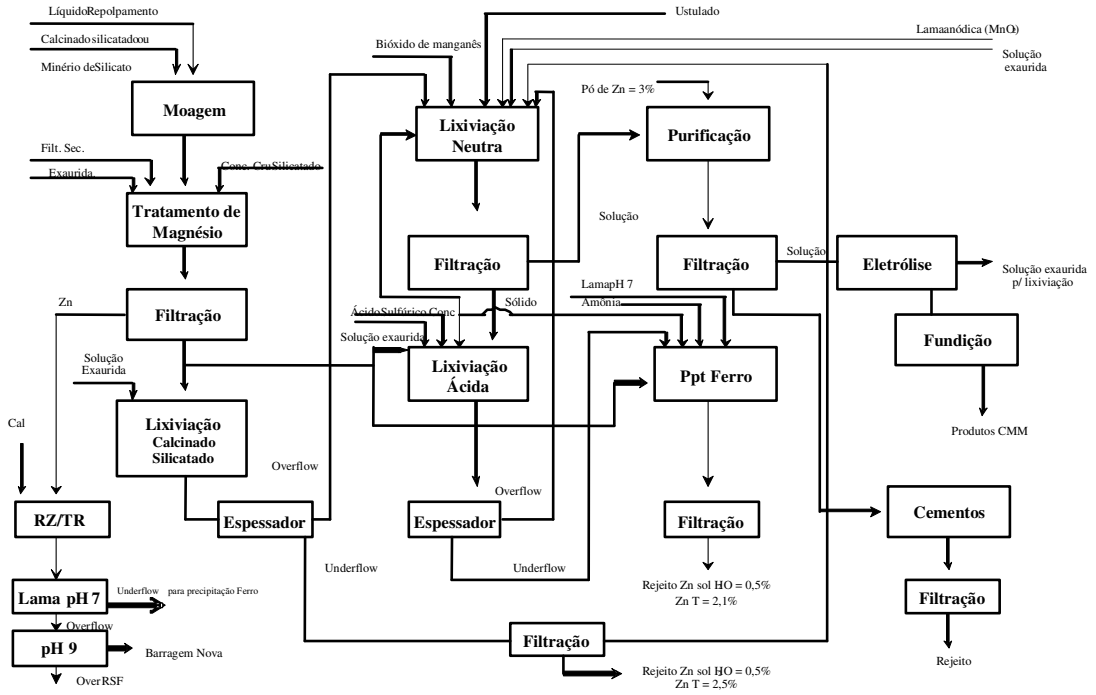

Figura 1.1 – Processo de Integração no tratamento de concentrados de silicatos e sulfetos de zinco (Souza, 2000).

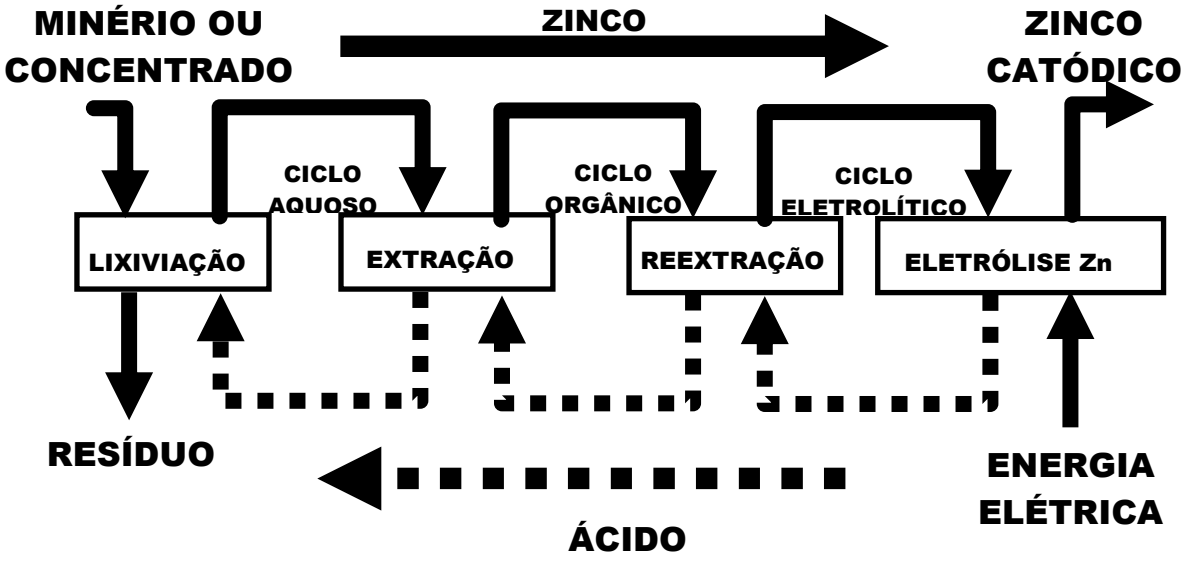

Figura 1.2 – Fluxograma resumido do processo MZP usando extração por solventes.

A cinética de dissolução de fontes de zinco não-sulfetadas tem sido bem menos estudada do que as de sulfetos do metal. Terry and Monhemius (1983) estudaram a cinética de lixiviação de hermimofita natural, bem como willemita sintética e natural. Os autores observaram que a dissolução em ácido era controlada por difusão para hemimorfita e reação química para a willemita. Abdel-Aal (2000), estudando a cinética de lixiviação de silicatos de zinco de baixo teor, propôs que o processo era controlado por difusão na camada de cinza com uma energia de ativação associada de 13.38 kJ/mol. Entretanto, não ocorria a formação de nenhum produto sólido durante a lixiviação do silicato de zinco, mas somente íons zinco e sílica foram produzidos, embora a última possa afetar as propriedades de transporte da solução, devido à elevação na viscosidade da mesma. O autor não apresentou uma explicação para o controle proposto por difusão na camada de produto. É possível que a difusão através dos poros do sólido seja uma explicação para os controles observados durante a lixiviação. Tem sido mostrado, que se o transporte através dos poros dos sólidos for a etapa controladora, uma expressão similar ao *modelo do núcleo não reagido* ("shrinking core model"- SCM) com controle por difusão pode ser obtida (Youcai and Stanforth, 2000).

Embora não haja referência à influência do ferro durante a lixiviação no processo integrado de tratamento de sulfetos e silicatos da Votorantim Metais Brasil, o interesse pelo processo hidrometalúrgico para tratar concentrado silicatado com elevado teor de ferro se tornou notável a partir da observação de que o plano de lavra da Mina de Vazante, no Brasil, indicava a ocorrência de elevados níveis do elemento no material a ser lavrado e que seria posteriormente submetido ao processo de flotação, anteriormente ao processo hidrometalúrgico da unidade de Três Marias.

Do ponto de vista acadêmico, é importante conhecer a influência do teor de ferro nos concentrados de silicato de zinco sobre a extração de zinco e a cinética de dissolução dos mesmos. Um novo conceito de tratamento de concentrados de silicato e sulfetos será apresentado visando à eliminação de impurezas e aumento da proporção de silicato no processamento de concentrados de zinco, podendo-se se obter um mix de até 100% concentrado silicatado na alimentação.

1.3. Objetivos e organização da tese

Considerando a matéria-prima (minérios e concentrados) como um dos itens mais importantes para a metalurgia do zinco e também a especificidade da indústria brasileira em tratar concentrados sulfetados e silicatados, esta tese tem os seguintes objetivos:

- Estudar a cinética de lixiviação, aplicando modelos cinéticos - do núcleo não reagido e do grão, de concentrados sulfetados e silicatados de zinco, determinando os valores de energia de ativação e ordem de reação para os reagentes utilizados na lixiviação de silicatos e sulfetos.

- Avaliar a lixiviação de concentrados silicatados com baixos e altos teores de ferro (até 9%), propondo uma rota tecnológica inovadora para o tratamento dos concentrados com elevados teores do elemento.

Neste sentido, a tese foi organizada em capítulos, sendo que no Capítulo 2 será apresentado o trabalho entitulado “The leaching kinetics of a zinc sulphide concentrates in acid ferric sulphate”. Neste artigo, será aplicado o modelo do núcleo-não reagido

("Shrinking Core Model - SCM"), com controle por reação química e difusão na camada de produto, e o método das velocidades iniciais, para descrever a cinética de dissolução do concentrado sulfetado.

No Capítulo 3, será apresentado o trabalho, entitulado "Kinetics study of the sulphuric acid leaching of a zinc silicate calcine". O tema central será a proposição de utilização do modelo do grão, para descrever o comportamento cinético da lixiviação de um concentrado calcinado de silicato de zinco, em meio sulfúrico.

No capítulo 4, o trabalho "The effect of the iron content in zinc silicate concentrate leaching with sulphuric acid", tratará da influência do teor de ferro na cinética de lixiviação do concentrado de silicato de zinco em meio sulfúrico. Um novo processo para o tratamento de concentrados silicatados com elevados teores de ferro, é proposto visando o tratamento exclusivo de concentrados silicatos, sem a necessidade de integração com tratamento de concentrados sulfetados. Uma versão modificada destes capítulos foi aceita para publicação no periódico Hydrometallurgy.

1.4. Referências

Abdel-Aal, E.A., 2000. Kinetics of sulfuric acid leaching of low-grade zinc silicate ore. Hydrometallurgy, 55(3): 247-254.

Boni, M. 2005. The geology and mineralogy of non-sulfide zinc ore deposits. In: Lead & Zinc '05. Y. Umetsu (ed.) Kyoto, Japan, TMS, Warrendale, PA. pp. 1299-1313.

Crundwell, F.K., 1988. The influence of the electronic structure of solids on the anodic dissolution and leaching of semiconducting sulphide minerals. Hydrometallurgy, 21: 155-190.

Dutrizac, J.E., 1992. The leaching of sulphide minerals in chloride media. Hydrometallurgy, 29: 1-45.

Dutrizac, J.E. 2005. The kinetics of sphalerite dissolution in ferric sulphate-sulphuric acid media. In: Lead & Zinc '05. Y. Umetsu (ed.) Kyoto, Japan, TMS, Warrendale, PA. pp. 833-851.

Feneau, C., 2002. Non-ferrous metals from Ag to Zn. Umicore, Brussels, 285 pp.
Markus, H., Fugleberg, S., Valtakari, D., Salmi, T., Murzin, D.Y. and Lahtinen, M., 2004. Kinetic Modelling of a solid-liquid reaction: reduction of ferric iron to ferrous iron with zinc sulphide. Chemical Engineering Science, 59: 919-930.
Perez, I.P. and Dutrizac, J.E., 1991. The effect of the iron content of sphalerite on its rate of dissolution in ferric sulphate and ferric chloride media. Hydrometallurgy, 26(2): 211-232.
Souza, A.D., 2000. Integration process of the treatment of concentrates or zinc silicates ore and roasted concentrate of zinc sulphides, WO 0046412.
Souza, A.D., Pina, P.S. and Leao, V.A., 2007. Bioleaching and chemical leaching as an integrated process in the zinc industry. Minerals Engineering, 20(6): 591-599.
Svens, K., Kerstiens, K. and Runkel, M., 2003. Recent experiences with modern zinc processing technology. Erzmetall, 56: 94-103.
Terry, B. and Monhemius, A.J., 1983. Acid dissolution of willemite ($(Zn,Mn)_2SiO_4$) and hemimorphite ($Zn_4Si_2O_7(OH)_2H_2O$). Metallurgical Transactions B - Process Metallurgy, 14(3): 335-346.
Youcai, Z. and Stanforth, R., 2000. Extraction of Zinc from Zinc Ferrites by Fusion with Caustic Soda. Minerals Engineering, 13(13): 1417-1421.

CAPÍTULO 2

THE LEACHING KINETICS OF A ZINC SULPHIDE CONCENTRATE IN ACID FERRIC SULPHATE

Abstract

This work examines the dissolution kinetics of a zinc sulphide concentrate in acid ferric sulphate medium. The effects of temperature, ferric ion and sulphuric acid concentrations, agitation speed and particle size on the leaching kinetics were investigated. The leaching process could be separated into two stages. Initially, the dissolution kinetics was controlled by the chemical reaction at the surface of the zinc sulphide particles followed by a second step where the reaction was controlled by diffusion of the reagents or products through the elemental sulphur (ash) layer. The activation energy of the chemical controlled step was 6.59kcal/mol (27.54kJ/mol) and the value determined for the diffusion controlled step was 4.68kcal/mol (19.56kJ/mol). The reaction order with respect to ferric ion and sulphuric acid concentrations were approximately 0.50 and 1.00, respectively. Analysis of the unreacted and reacted sulphide particles by SEM-EDS showed a progressive increase of the thickness of the elemental sulphur layer on the solid surface. The development of this sulphur layer is further evidence of the change on the rate-controlling step as the reaction progress.

Keywords: chemical leaching, sphalerite, sulphur, reaction order

2.1. Introduction

The route *Roasting, Leaching, Electrolysis (RLE)* has been the main process of producing metallic zinc since 1916 and is currently responsible for more than 85% of the total zinc production (Souza et al., 2006). Notwithstanding, the RLE route has many restrictions to treat zinc concentrates high in silica, calcium, copper and iron. Also, the prevention of SO_2 emission from the process and marketing of sulphuric acid are challenging the future of this technology (Deller, 2005).

Over the last few years, several innovative leaching processes have been proposed, such as, bioleaching and chemical leaching as an integrated process (Souza et al., 2006), persulphate leaching (Babu et al., 2002), heap bioleaching (Lizama et al., 2003; Madhuchbanda et al., 2003), sulphide and silicate leaching integration (Souza, 2005) and solvent extraction for zinc recovery from oxide ores (Garcia et al., 2000). Some of these innovations have made the zinc industries more competitive. Others, however, require further development. For instance, the Três Marias Zinc Plant (Votorantim Group in Brazil) is in the first quartile of lowest metallurgical costs as it uses a new technology integrating sulphide and silicate concentrate treatment. Likewise, Skorpion Zinc (Anglo American Group), in Namibia, has started its solvent extraction technology and it is expected to be the metal producer with the lowest cost (Brook Hunt, 2005).

Regarding chemical leaching, two similar routes were proposed in the 1970's to produce zinc as a substitute for the RLE process: (i) *Direct Atmospheric Leaching* (Svens et al., 2003) in which zinc sulphide concentrates are leached directly with a ferric ion solution; and (ii) *Pressure Leaching* that adopts a similar approach (Baldwin

et al., 1995), except that leaching is carried out in autoclaves (14-15atm oxygen pressure).

The kinetics of ferric ion leaching of sphalerite concentrates has been described by several authors (Dutrizac, 1992; Dutrizac, 2005; Markus et al., 2004; Palencia Perez and Dutrizac, 1991). It is agreed that elemental sulphur is the main oxidation product and the iron content plays a key role during leaching. Many authors have observed that temperature increases the leaching rate, however the reported values of activation energy varies widely (Palencia Perez and Dutrizac, 1991). Furthermore, the effect of acid concentration on zinc dissolution is also well characterized but the reaction order with respect to the sulphuric acid concentration has been determined only by few researchers (Crundwell, 1988).

The objective of this work was to assess the effects of some parameters such as temperature (40 - 90ºC), ferric ion concentration (0.10 - 1.00mol/L), particle size, sulphuric acid concentration (0.25 - 1.00 mol/L) and agitation speed (240 - 600min.$^{-1}$) on the dissolution kinetics of a zinc sulphide concentrate. The Shrinking Core Model (SCM) with chemical reaction control and product layer diffusion control as well as the initial rate (IR) method were used to describe the dissolution kinetics of this concentrate.

2.2. Reaction Model

The leaching of zinc sulphide in ferric sulphate solutions includes a heterogeneous reaction represented by:

$$Fe_2(SO_4)_{3\,(aq)} + ZnS_{\,(s)} \rightarrow 2FeSO_{4\,(aq)} + ZnSO_{4\,(aq)} + S^{\circ}_{(s)} \qquad (2.1)$$

A major feature of this system is that the chemical reaction step and mass transport are coupled in series. Besides, one may assume that the solid particle retains its initial shape and that the chemical reaction occurs in a sharp interface between the original solid and the reaction product. Further assuming that the zinc sulphide particles have a spherical geometry and the chemical reaction is the rate-controlling step, the following expression of the shrinking core model can be used to describe the dissolution kinetics of the process (Levenspiel, 1999):

$$1-(1-\alpha)^{\frac{1}{3}} = K_R.t\,, \quad K_R = \frac{b.k_s.[Fe(III)]^n}{\rho_{ZnS}.r_o} \qquad (2.2)$$

Similarly, when the diffusion of ferric ion through the elemental sulphur layer is the rate-controlling step, the following expression of the shrinking core model can be used to describe the dissolution kinetics (Levenspiel, 1999):

$$1-3(1-\alpha)^{\frac{2}{3}} + 2(1-\alpha) = K_D.t \text{ , where } K_D = \frac{6.b.D_{eff}.[Fe(III)]}{\rho_{ZnS}.r_o^{\,2}} \qquad (2.3)$$

Where: α = the fractional conversion, K_R = kinetic parameter for reaction control, K_D = kinetic parameter for product diffusion control, b = stoichiometric coefficient (0.50 in this case – reaction (2.1)), k_s = chemical reaction rate constant, [Fe(III)] = ferric ion concentration, ρ_{ZnS} = molar density of ZnS, r_0 = particle radius; n = order of reaction with respect to Fe(III) and D_{eff} = effective diffusion coefficient.

When the chemical reaction is the rate controlling-step a plot of $1-(1-\alpha)^{\frac{1}{3}}$ versus time is a straight line with a slope of K_R. If the process is controlled by diffusion through the solid product layer a plot of $1-3(1-\alpha)^{\frac{2}{3}}+2(1-\alpha)$ versus time is also a straight line whose slope is K_D (Levenspiel, 1999).

In order to compare the values of activation energy and reaction order obtained from equations (2.2) and (2.3) the initial rate of the zinc sulphide dissolution was determined at different temperatures and ferric ion concentrations. The initial rate parameters were determined by fitting the experimental data to a hyperbolic equation:

$$[Zn]=\frac{k_1.t}{k_2+t} \tag{2.4}$$

Where: [Zn] = zinc concentration, t = time, k_1 and k_2 = constants.

The initial dissolution rate is the slope of equation (2.4), at t = 0. That means the ratio between k_1 and k_2 ($k_1 / k_2 = K$), since the first derivate of equation (2.5) is:

$$\frac{d[Zn]}{dt}=\frac{k_1.k_2}{(k_2+t)^2} \tag{2.5}$$

and for all purposes, K can be written as $K = A.k.[Fe^{3+}]^n$ where A stands for area of reaction, k for a Arrhenius temperature dependent constant, $[Fe^{3+}]$ for the ferric ion concentration and n for order of reaction.

2.3. Experimental

Table 2.1 presents the chemical analysis of the bulk concentrate. Before leaching, the concentrate was dry-ground and wet-sieved to yield a particle size distribution between 210μm and 38μm. The zinc, iron and sulphur content of the different particle size fractions of the zinc sulphide concentrate are presented in table 2.2. Average zinc and iron concentrations are 48% and 12%, respectively.

Table 2.1 – Chemical analysis of the bulk zinc sulphide concentrate.

%Zn	%S	%Fe	%Cd	%Cu	%Co	%Pb
48.13	31.02	12.12	0.21	0.95	0.002	1.28

Table 2.2 – Chemical analysis (Zn, Fe and S) of different screened fractions of zinc sulphide concentrate.

Size fraction	%Zn	%S	%Fe
210-150 μm	49.52	32.57	10.91
150-105 μm	49.46	32.28	11.36
105-75 μm	48.13	32.63	12.57
75-53 μm	49.20	32.93	11.11
53-45 μm	48.69	31.95	12.10

The mineralogical analyses of the concentrate were carried out by SEM-EDS. The samples were coated with graphite by electro-deposition, using a Jeol JEE 4C instrument and observed in a JEOL JSM 5510 scanning electron microscope (SEM) with an accelerating voltage 0.5 – 30kV and equipped with a spectrometer for micro-

analysis based on a energy dispersive x-ray spectroscopy system (EDS). Sphalerite is the main mineral phase and pyrite, quartz and galena were also present in minor quantities. Table 2.3 presents the electron microprobe analysis of isolated sphalerite particles. The difference between the iron content observed by chemical (table 2.2) and EDS analysis (table 2.3) is due to the presence of small quantities of pyrite in the zinc concentrate. In addition, table 2.4 presents the values of surface area, micro pores volume and micro pores area determined by nitrogen adsorption-desorption isotherm obtained from a Nova 1000 High Speed Gas Sorption Analyser (*Quantachrome*). The trends of surface area follow that of the particle porosity. A large sample (~4.0g) was used and the Nova 1000 parameters: equilibration tolerance, time to remain in tolerance and maximum equilibration time were set at 0.05, 360 and 720, respectively, to improve the accuracy of the low surface area measurements.

Table 2.3. EDS analysis (Zn, S and Fe) of the zinc sulphide concentrate (average of 10 points).

Element	EDS analysis
Zn	59.48
S	31.89
Fe	8.55

Table 2.4. Surface parameters of different screened fractions of zinc sulphide concentrate.

Size fraction	Surface area (m^2/g)	Micro pores volume (cm^3/g)	Micro pores area (m^2/g)
210-150 μm	0.882	$3.408x10^{-3}$	1.060
150-105 μm	0.556	$2.416x10^{-3}$	0.734
105-75 μm	0.765	$2.834x10^{-3}$	1.035
75-53 μm	0.829	$2.923x10^{-3}$	1.092
53-45 μm	0.690	$3.521x10^{-3}$	0.899
45-38 μm	0.800	$3.804x10^{-3}$	1.089

The chemical leaching experiments were carried out batchwise in a closed water-jacket borosilicate glass reactor with 750mL total volume. The solution volume was 500mL and the solid concentration 0.5% (w/v). Agitation was provided by a magnetic stirrer because mechanical stirring showed similar results but higher evaporation losses. Leaching solutions were prepared using reagent grade chemicals ($Fe_2(SO_4)_3.5H_2O$ and H_2SO_4, *Synth*) and distilled water. At selected time intervals, a known amount (3mL) of slurry was withdrawn and filtered. For every sample taken from the reactor, an equal volume of blank solution was returned to the vessel so that the experiments were carried out at constant volume. The zinc extraction was determined by analyzing zinc concentration in solution (Atomic Absorption Spectrometry, Perkin Elmer AAnalyst 100).

Scanning electron microscopy (SEM) was used to examine the morphology of the leaching residues. The samples were coated with graphite by electro-deposition, using a

Jeol JEE 4C instrument and observed in a JEOL JSM 5510 scanning electron microscope (SEM), with an accelerating voltage 0.5 – 30kV, equipped with a spectrometer for micro-analysis based on a Energy dispersive x-ray spectroscopy system (EDS).

2.4. Results and discussion

2.4.1. Effect of agitation speed

Figure 2.1 presents the effect of stirring speed on zinc extraction. The increase of stirring speed in the range of 240-600rpm does not increase the zinc extraction. Therefore, the dissolution process does not seem to be controlled by mass transfer through the liquid boundary film. Therefore, in all the posterior experiments, the stirring speed was kept at 480 rpm.

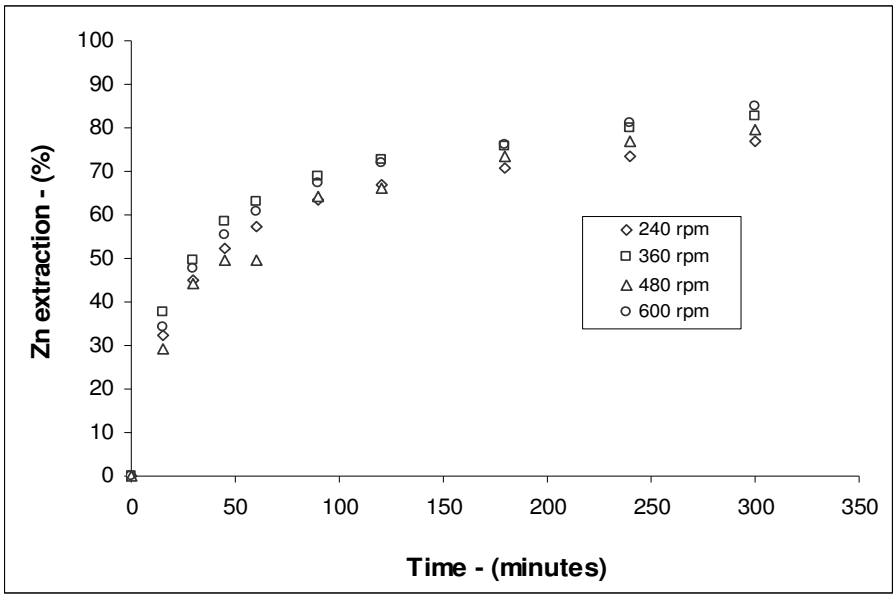

Figure 2.1 – Effect of stirring speed on the zinc extraction. Temperature 70ºC, 1.0mol/L H_2SO_4, 0.5mol/L Fe(III), 0.5% solids (w/v) and particle size 75-53µm.

2.4.2. Effect of temperature

Figure 2.2 shows the change on zinc extraction with the leaching time as function of temperature in the range of 40ºC to 90ºC. These results show that temperature has a major role on the zinc dissolution process. The zinc extraction is relatively low in the experiments carried out at 40ºC (45%) but significantly increases as the leaching temperature rises and a high zinc extraction was observed at 90ºC (90%). Similar results were observed by Dutrizac and MacDonald (1978), Bobeck and Su (1985) and Aydogam et al. (2005) in leaching experiments carried out in ferric chloride solutions; by Palencia Perez and Dutrizac (1991) and Dutrizac (2005) in studies performed in ferric sulphate medium; and by Babu et al. (2002) with ammonium persulphate solutions.

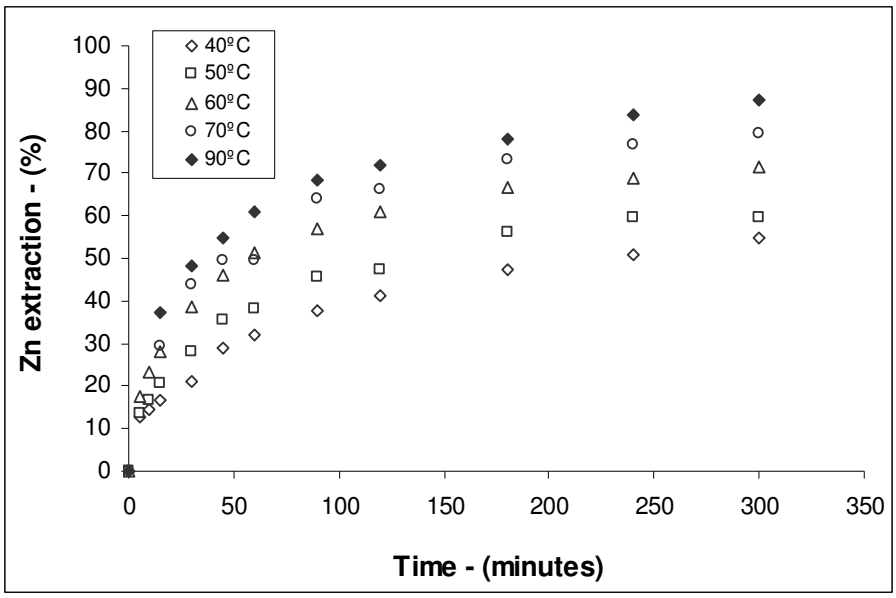

Figure 2.2 – Effect of leaching temperature on the zinc extraction. 1.0mol/L H_2SO_4, 0.5 mol/L Fe(III), 0.5% solids (w/v), agitation speed 480rpm and particle size 75-53µm.

2.4.3. Effect of acid concentration

Figure 2.3 presents the effect of sulphuric acid concentration upon the zinc extraction as function of leaching time at a constant Fe(III) concentration. It can be seen, that zinc extractions increase gradually with the leaching time and sulphuric acid concentration indicating that an appreciable quantity of zinc sulphide could be dissolved by sulphuric acid (Dutrizac, 2005). The direct acid dissolution of zinc sulphide produces H_2S, in the absence of oxygen, rather than elemental sulphur. Nevertheless, as there was no solution degassing in the present work, the equation (2.6) has likely took place despite a weak hydrogen sulphide smell in the beginning of the experiments:

$$ZnS + H_2SO_4 + 1/2O_2 = ZnSO_4 + S^o + H_2O \quad (2.6)$$

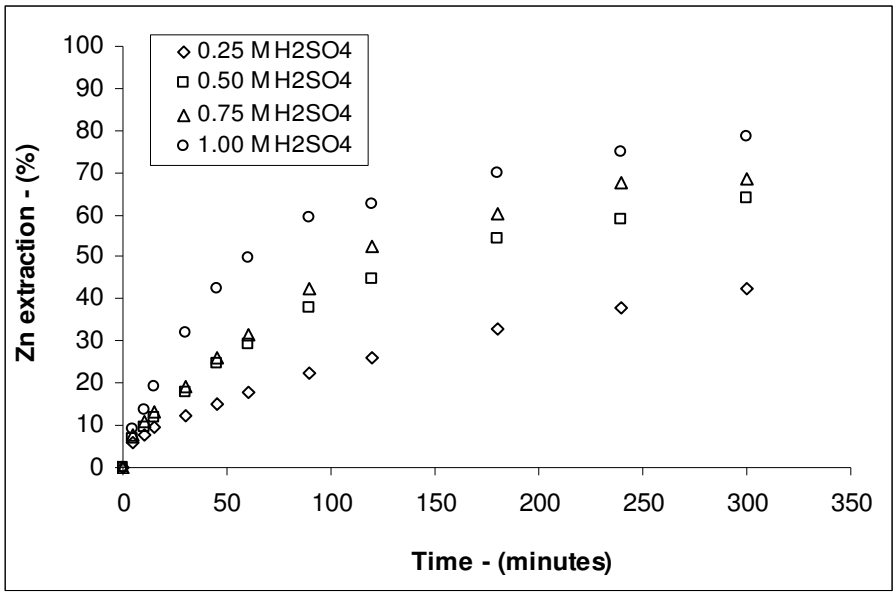

Figure 2.3 – Effect of sulphuric acid concentration on zinc extraction. Temperature 70ºC, 0.5mol/L Fe(III), 0.5 %solids (w/v), agitation speed: 480rpm and particle size 75-53µm.

Dutrizac (2005) studied the effect of sulphuric acid concentration upon sphalerite dissolution in ferric sulphate medium. The author observed that the zinc dissolution kinetic parameters, determined by the shrinking core model with chemical reaction control, were independent of acid concentration for acid concentrations smaller than 0.10mol/L since the hydrolysis of ferric sulphate produced acidity by itself. However, for acid concentration above 0.10mol/L, the dissolution rate increases with the latter. Dutrizac (2005) attributed the faster kinetics to the existence of a parallel dissolution reaction involving H_2S acid production and its subsequent oxidation by Fe(III), as represented by equations (2.7) and (2.8). If the acid dissolution plays a key role during the zinc sulphide dissolution, the elemental sulphur produced was not stuck at the particle surface. In contrast, the SEM/EDS analysis showed the existence of an elemental sulphur layer covering the particles during the leaching process. Similarly, Babu et al. (2002) also verified that the zinc extraction is function of sulphuric acid concentration, in experiments carried out in ammonium persulphate solutions.

$$ZnS + H_2SO_4 = ZnSO_4 + H_2S \quad (2.7)$$

$$Fe_2(SO_4)_3 + H_2S = 2FeSO_4 + H_2SO_4 + S^o \quad (2.8)$$

2.4.4. Effect of particle size

Figure 2.4 presents the effect of the concentrate particle size on zinc extraction. The decrease in particle size enhanced the zinc dissolution, but it can be seen that particle size plays a minor role in the leaching process. The zinc extraction observed in the experiment carried out with the particle size between 38-45μm is only around 10% higher than that achieved in the experiment performed with particle size in the range of

210-150µm. The small difference observed is, probably, due to the negligible increase of solid surface area (BET surface area) with decreasing particle sizes as an effect of porosity and natural cracks (table 2.4 and figure 2.5). Porosity of the concentrate would not be a factor in the shrinking core model (SCM) applied to these experiments since it takes into consideration a sharp interface reaction. However, reactant porosity plays an important role if the reaction interface is diffuse, meaning that the oxidation reaction proceeds inside the pores. Massaci et al. (1998) also verified the non-significance of the effect of particle size in a factorial experiment carried out with a zinc sulphide ore in ferric sulphate media. The authors credited this behaviour to the presence of a natural porosity in the structure of the zinc sulphide particles (as observed in the present work, figure 2.5), but surface area and porosity data were not presented. Another important factor that must be considered is the high reactivity of sphalerite that could have reduced the effect of particle size upon the zinc extraction (Aydogan et al., 2005; Bobeck and Su, 1985; Ghosh et al., 2002; Silva, 2004).

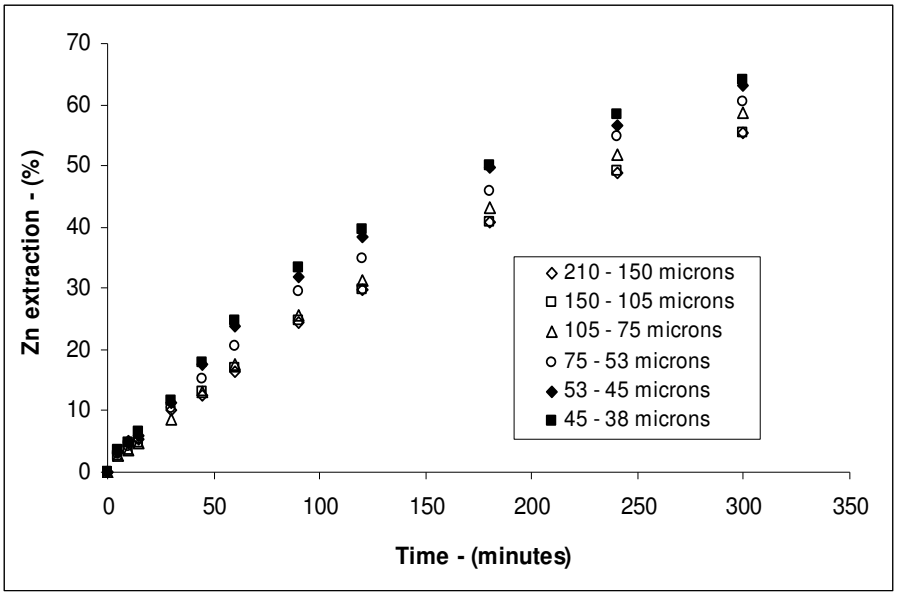

Figure 2.4 – Effect of particle size upon the zinc extraction. Temperature 50ºC, 0.25mol/L Fe(III), 0.25mol/L H_2SO_4, 0.5% solids (w/v) and agitation speed: 480rpm.

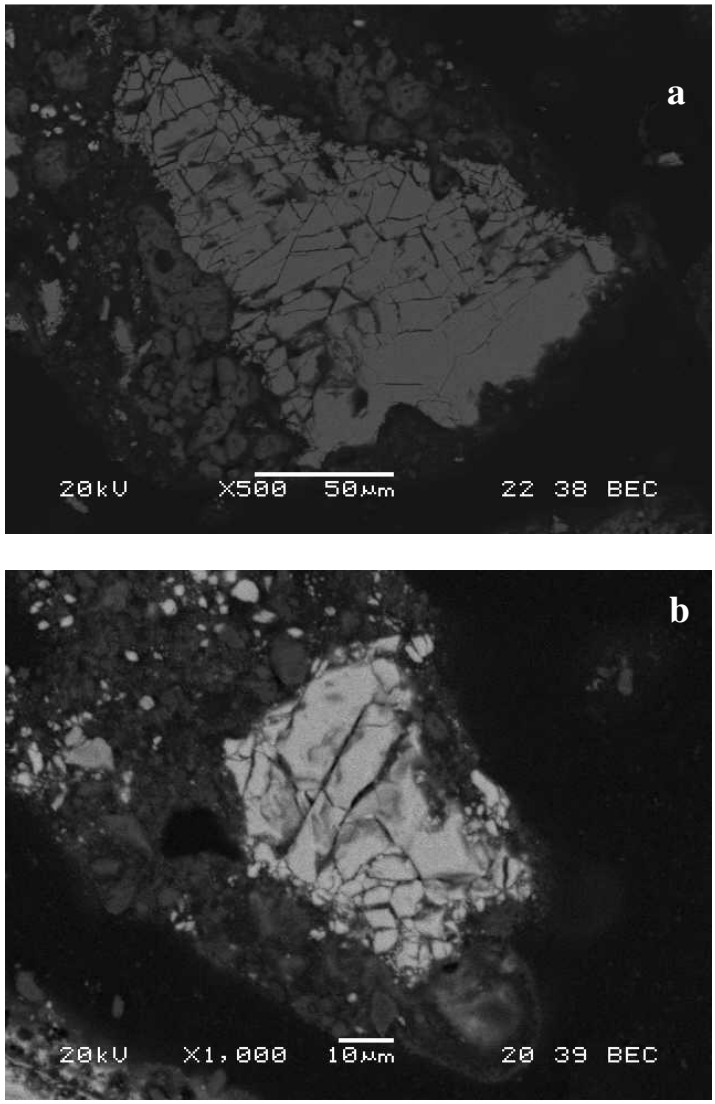

Figure 2.5 – Particles of zinc sulphide concentrate showing small fractures throughout the samples (a) 500X, (b) 1000X.

2.4.5. Effect of ferric ion concentration

Ferric ion is a powerful oxidant used in the dissolution processes of several metallic sulphides such as: chalcopyrite, covellite, bornite, sphalerite, etc. The leaching reaction directly involves ferric ions, and it would be expected that the ferric sulphate concentration would have an important role in the zinc sulphide dissolution process. Figure 2.6 presents the effect of ferric ion concentration on zinc extraction as function

of leaching time. It can be noticed that zinc extraction increases gradually with the leaching time and ferric ion concentration which is consistent with that observed by Dutrizac and MacDonald (1978), Palencia Perez and Dutrizac (1991), Aydogam et al. (2005) and Dutrizac (2005).

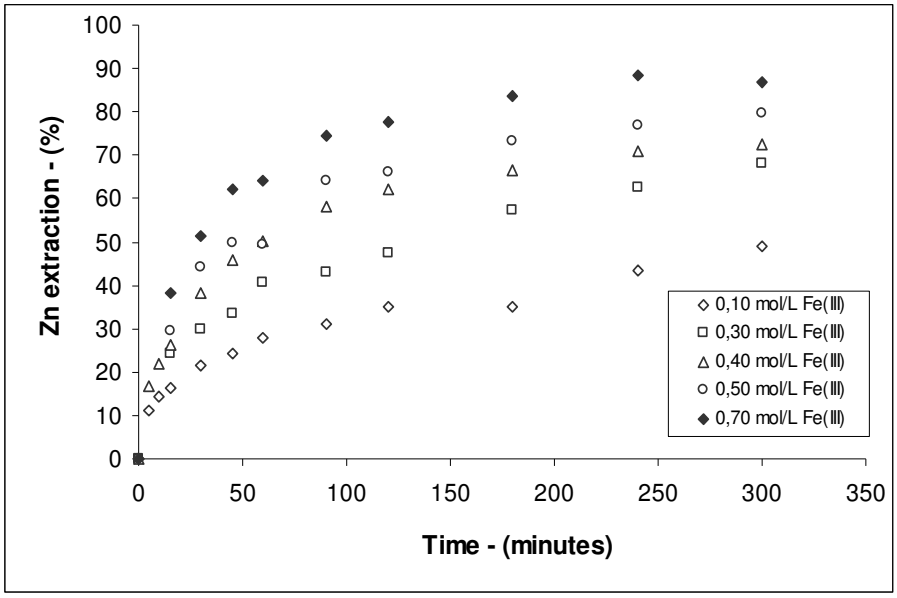

Figure 2.6 – Effect of ferric iron concentration on the zinc extraction. Temperature 70ºC, 1.0mol/L H_2SO_4, 0.5% solids (w/v), agitation speed 480rpm and particle size 75-53µm.

2.4.6. Morphology of the leaching residues

The morphology of the zinc sulphide concentrate before and after leaching was examined by SEM-EDS (figure 2.7). The particles of the zinc sulphide concentrate before the leaching process present a clear surface and have approximately the same form and size (figure 2.7 (a)). After the leaching progress, the micrographs of the leaching residues show a progressive increase in the roughness of the solid and also an increase in the amount of elemental sulphur covering the particle surfaces (figures (2.7(b) to 2.7(f)). After 45% zinc extraction (figure 2.7(d)), the particles present their

surface completely covered by an elemental sulphur layer, as proposed previously by Bobeck and Su (1985) and Crundwell (1987).

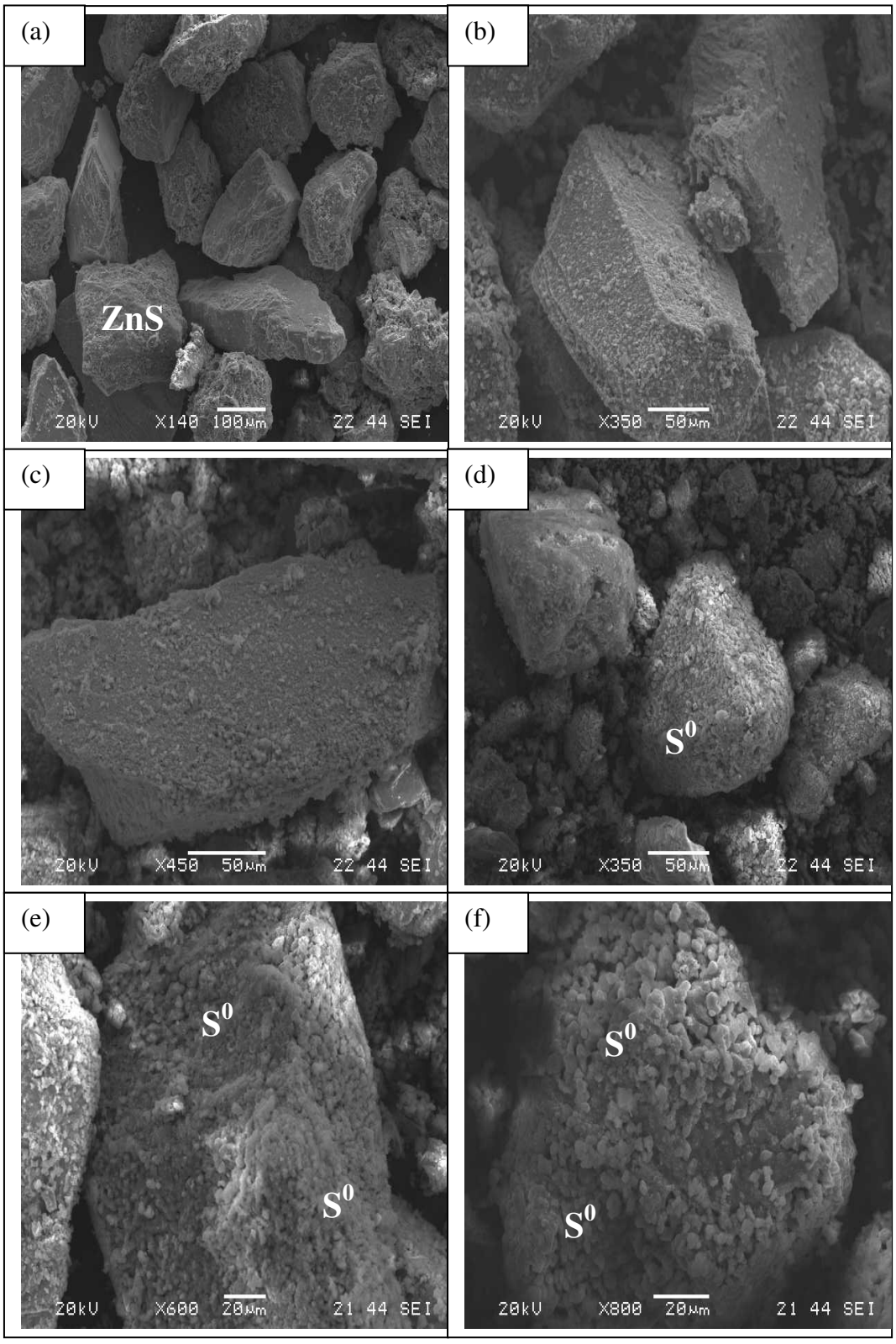

Figure 2.7. (a) Particles of zinc sulphide concentrate before leaching; (b) after 10% of zinc extraction; (c) after 25% of zinc extraction; (d) after 45% of zinc extraction; (e) after 60% of zinc extraction. (f) after 80% of zinc extraction.

2.4.7. Kinetics analysis

Dutrizac and MacDonald (1978) proposed that, during the oxidative leaching of ZnS, elemental sulphur would be formed preferably than sulphate, according the equation (2.1). The authors also determined that around 85% to 95% of the sulphide is oxidized into elemental sulphur. During the initial step of dissolution, the quantity of elemental sulphur produced is very low so that the diffusion resistance is small. As reaction proceeds, sulphur covers the zinc particle (figure 2.8) and as this layer increases in thickness, the diffusion of reagents or products through it may become the rate-controlling step. Therefore, it may not be reasonable to consider that just one step, chemical reaction or diffusion through the elemental sulphur layer, would control the entire process.

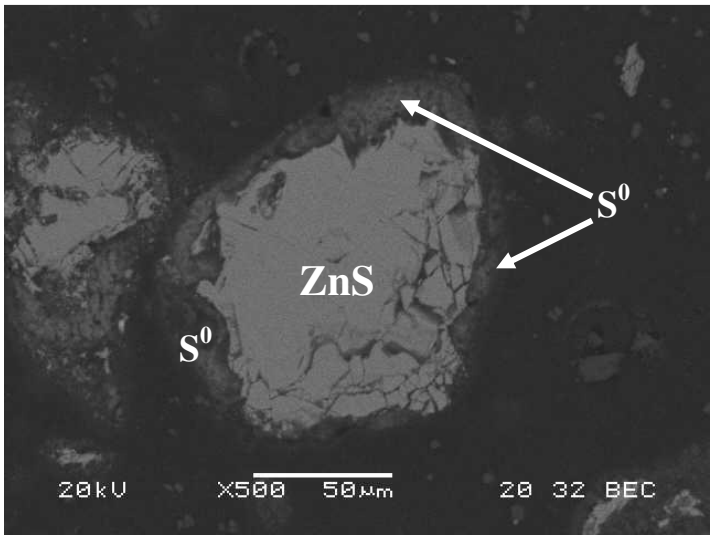

Figure 2.8. Partially oxidized zinc sulphide particle showing an elemental sulphur layer around a ZnS core, after 40% of zinc extraction.

Equations (2.2) and (2.3) can be used to describe the zinc dissolution process when only one step, chemical reaction or diffusion through the reaction product, controls the entire

process. However, as stated before, during ferric sulphate leaching of sphalerite, it is observed that the elemental sulphur produced during the sulphide dissolution has an important role in the final stages of leaching (Bobeck and Su, 1985; Crundwell and Verbaan, 1987; Silva, 2004) so that a model that considers both the chemical reaction and diffusion of ferric ion through the elemental sulphur layer would be more realistic. If the chemical reaction is first-order with respect to ferric ion concentration the model is constructed by the addition of the terms that represent the resistances due to chemical reaction and diffusion, since they act in series and are linear in concentration. This approach was used by Bobeck and Su (1985) to describe the leaching of sphalerite in ferric chloride solution. In a recent work, Silva (2004) also used the same approach to study the leaching of zinc sulphide in ferric sulphate solution, although the process was not linear in concentration since a reaction order of 0.50 with respect the ferric ion concentration was determined by the author. Therefore, the simple addition of the resistance terms, as used by Silva (2004), although can produce a mixed control model that fits well the experimental results, is physically biased. Unfortunately, the mathematical solution for mixed control, considering fractionary reaction orders usually requires a numerical solution. A different approach was used by Weisener et al. (2003) that observed two distinct rate regimes for the sphalerite leaching in perchloric acid solutions: a fast rate followed by a slow one. The authors attributed the decrease in the zinc dissolution rate to the formation of a thick continuous metal-deficient polysulfide surface layer, which was formed during the fast initial leaching phase and reached a steady state thickness in the subsequent slow rate stage. Unlike other studies, Weisener et al. (2003) did not consider that the presence of an elemental sulphur layer contributes to any noticeable effect on the leaching rate. This behaviour was also noticed by other authors modelling sphalerite chemical kinetics such as Bobeck and Su (1985),

Crundwell (1987). The approach was to split the extraction curve in two different segments and to perform a piecewise fitting to a chosen SCM limiting case.

The approach used Weisener et al. (2003) and other authors was also used in the present work. 40% zinc extraction was chosen as the value where the kinetics changed from chemical to diffusion control. Figure 2.8 shows a mineral particle with an elemental sulphur layer covering a ZnS core, after 40% zinc extraction. The whole particle was covered by an elemental sulphur layer which is consistent with the proposed change in the kinetics regime at this zinc extraction.

Figure 2.9 shows that the shrinking core model with reaction control fits the experimental data in the initial part of leaching (up to 40% of zinc extraction). Also, figure 2.9 shows that the shrinking core model with product diffusion control fits the experimental results in the final stages of leaching in agreement with the results observed by Crundwell (1987) and Bobeck and Su (1985) that verified that the sphalerite leaching by ferric chloride was chemically controlled in the initial stages of the process and later by diffusion in the product layer. The morphological analysis of the leaching residues (figure 2.7) reinforces the assumption that the zinc dissolution process is controlled by chemical reaction at initial stages and by diffusion through the elemental sulphur layer at later stages.

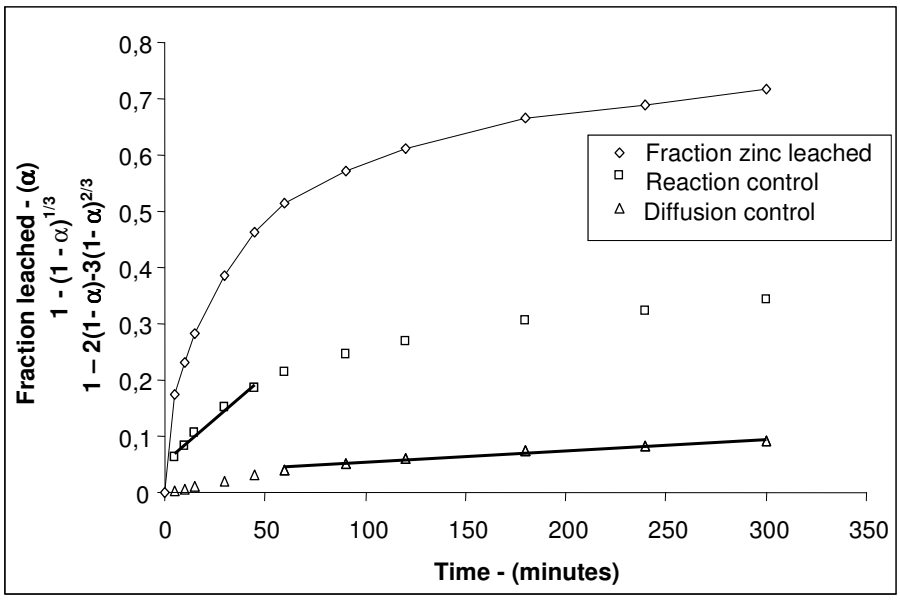

Figure 2.9 – Fitting of the shrinking core model to the experimental data. Temperature 60ºC, 1.0mol/L H_2SO_4, 0.5mol/L Fe(III), 0.5% solids (w/v), agitation speed 480rpm and particle size 75-53μm.

Temperature has an important effect on the dissolution rate of sphalerite and, as expected, an increase in the temperature causes an elevation in the dissolution rate. The reaction rate dependence on the temperature follows the Arrhenius equation (Levenspiel, 1999). This influence is expressed by the activation energy of the reaction. In general, a high value of activation energy indicates that the process is "strongly" influenced by temperature and therefore the rate-controlling step would be the reaction at the mineral surface. Conversely, a low value of activation energy indicates that the process is "weakly" influenced by the temperature and the rate-controlling step could be the mass transport of reagents or products through the reaction product (Levenspiel, 1999). Figure 2.10 presents the Arrhenius plot constructed with the rate constants values, K_R and K_D, calculated from equation (2.2) and (2.3) and the initial dissolution rate values, V_0, determined from equation (2.4). The values of K_R were calculated using data of the initial stages of dissolution (up to 40% of zinc extraction) while the values of

K_D were obtained from data coming from the later stages (above 40% of zinc extraction). The activation energy observed in the chemical reaction controlled step is 6.59kcal/mol (27.54kJ/mol) and the value determined in the product diffusion controlled step is 4.68kcal/mol (19.56kJ/mol). The activation energy calculated by the initial rate method is 6.00kcal/mol (25.08kJ/mol), similar to the value determined by the SCM assuming chemical reaction controlled step. The activation energy regarding the initial step of dissolution is higher than that observed for the final stages of leaching, which is in agreement with a chemical reaction controlling step followed by a product diffusion controlling step, as presented in figure 2.9. This similarity would be expected because in the initial stages of leaching, the elemental sulphur layer is very fine or nonexistent. Therefore, the activation energy value calculated with the K_R and V_0 represents the apparent activation energy for the zinc sulphide dissolution reaction. The value of activation energy determined in this work is smaller than those obtained previously, as shown in Table 3.. Very low values of apparent energy of activation can be associated to a reaction mechanism including adsorption of reactants followed by chemical reaction itself. Furthermore, it must be mentioned that the activation energy decreases at higher iron contents in the mineral (Bobeck and Su, 1985; Palencia Perez and Dutrizac, 1991).

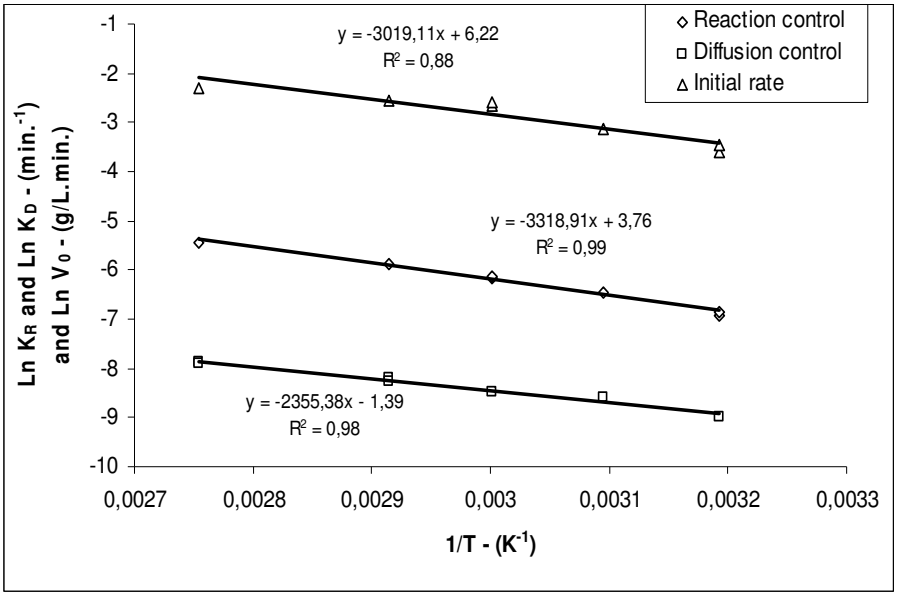

Figure 2.10. Arrhenius plots. 1.0mol/L H_2SO_4, 0.5 mol/L Fe(III), 0.5% solids (w/v), agitation speed 480rpm and particle size 75-53μm.

From the analysis through the shrinking core model with chemical reaction control (equation (2.2)) and with product diffusion control (equation (2.3)), there is a clear dependence of the model constants, K_R and K_D, on particle size. According to the SCM, leaching kinetics for a diffusion-controlled step is related to the inverse square of initial particle radius (r_0), while those processes controlled by chemical reaction show that K_R varies with the inverse of the initial particle radius. Figure 2.11 presents the plot of K_R versus $1/r_0$ and K_D versus $1/r_0^2$, respectively. It can be seen from the figure 2.11 that both rate constants (K_R and K_D) produced a linear relationship with the particle size terms ($1/r_0$ and $1/r_0^2$), further supporting the assumption of chemical reaction control during the initial stages and by diffusion in the elemental sulphur product layer during the later stages of dissolution.

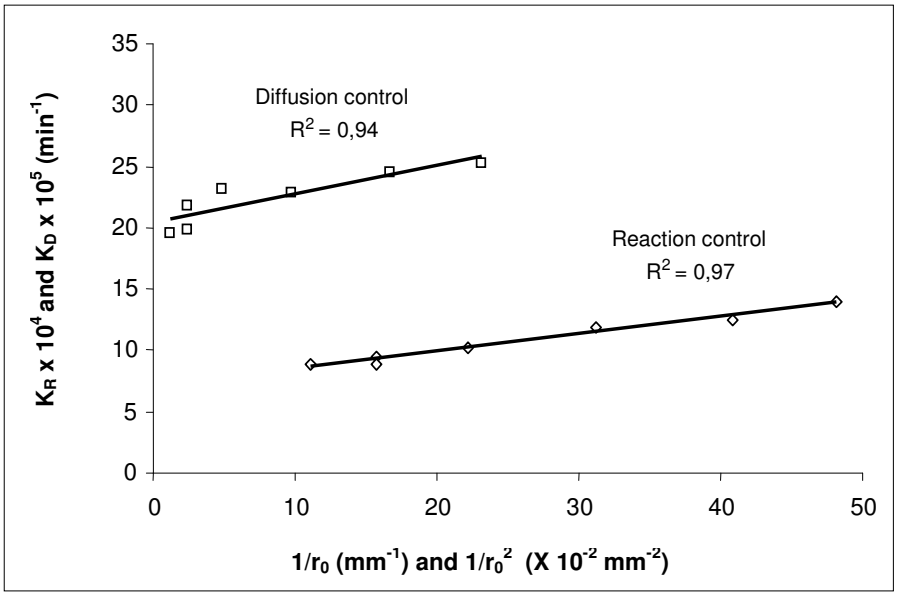

Figure 2.11. Plot of K_R and K_D versus $1/r_0$ (reaction control) and $1/r_0^2$ (diffusion control), respectively. Temperature 50ºC, 0.25mol/L Fe(III), 0.25mol/L H_2SO_4, 0.5% solids (w/v) and agitation speed: 480rpm.

The results of the experiments carried out with different ferric ion concentrations were also fitted to the shrinking core model with chemical reaction control (equation (2.2)) and with the hyperbolic function (equation (2.4)) so that the K_R an V_0 values could be estimated and used to determine the reaction order with respect the Fe(III) concentration. Figure 2.12 shows the Log versus Log plot from which the reaction order with respect to ferric ion concentration was determined from both K_R and V_0 values. As it is seen the reaction order determined by both methods (0.54 and 0.55 from the initial rate and shrinking core model, respectively) are similar and close to 0.50 and similar to those values available for the oxidative leaching of base metal sulphides (Aydogan et al., 2005; Dutrizac, 2005; Dutrizac and MacDonald, 1978; Rath et al., 1988). Similarly, Figure 2.13 presents the effect of sulphuric acid concentration on the K_R and V_0 values. From these values, the reaction orders were determined by both the initial rate method

and the SCM with chemical reaction control showing values around 1.00 which are consistent with those showed by Crundwell and Verbaan (1987), Dutrizac (2005), Dutrizac and MacDonald (1978). Babu et al. (2002) also observed the dependence of the zinc sulphide leaching rate with the sulphuric acid concentration. However, the authors did not determine the reaction order with respect to this reagent.

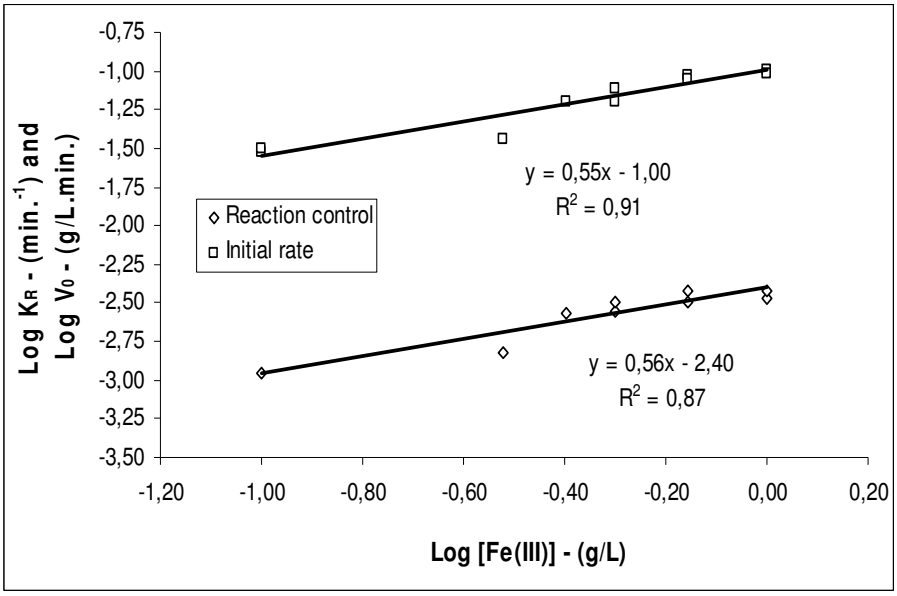

Figure 2.12. Plot of K_R and V_0 with the Fe(III) concentration. Temperature 70ºC, 1.0mol/L H_2SO_4, 0.5% solids (w/v), agitation speed: 480rpm and particle size 75-53µm.

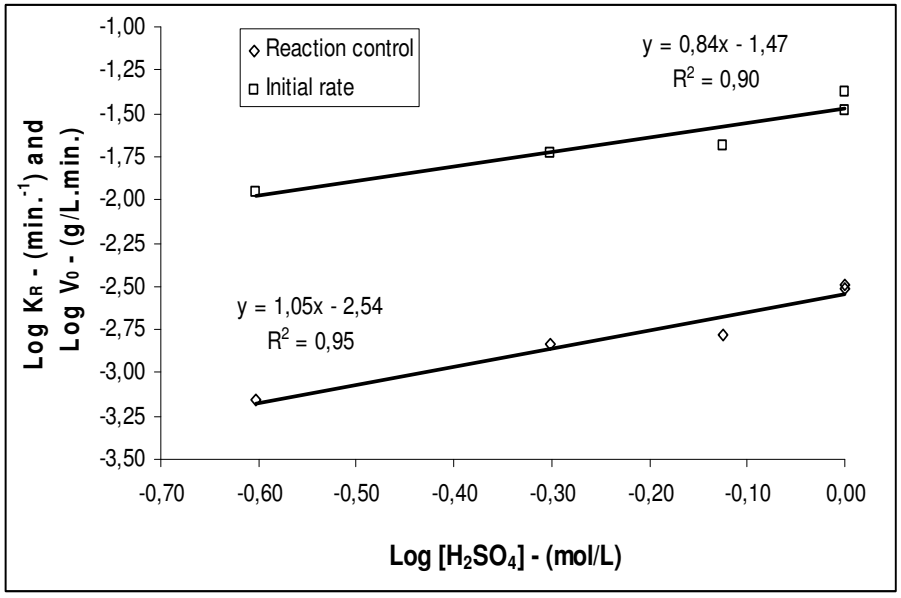

Figure 2.13. Plot of K_R and V_0 values with the H_2SO_4 concentration. Temperature 70ºC, 0.5mol/L Fe(III), 0.5% solids (w/v), agitation speed 480rpm and particle size 75-53µm.

2.5. Conclusions

In the present study, the dissolution kinetics of sphalerite in acidic ferric sulphate solution was studied. It was found that the zinc extraction increases with the increase in ferric ion concentration, temperature and sulphuric acid concentration. The decrease in the particle size enhanced zinc dissolution, but played only a marginal role in the leaching processes. This is probably due to the porosity and natural cracks of the solid, which increased surface area even at higher particle size. The shrinking core model with reaction control fitted the experimental data in the initial part of leaching (up to 40% of zinc extraction) and the shrinking core model with diffusion control fitted the experimental results in the final stages of leaching. The analysis of the zinc sulphide particles before and after leaching carried out by SEM-EDS supported the observed change of control. The particles presented a surface completely covered by an elemental sulphur layer after 40-50% zinc extraction.

The observed reaction orders were 1.00 and 0.50 with respect to sulphuric acid and ferric ion concentrations, respectively. The apparent activation energy determined in the chemical reaction controlled step was 6.59kcal/mol (27.54kJ/mol) and the value obtained for the diffusion controlled step was 4.68kcal/mol (19.56kJ/mol). As the activation energy found in the initial phase of dissolution process is higher than the value observed in the final stages of leaching it reinforces that the process is chemically controlled during the initial stage and diffusion controlled at the final stage of leaching.

2.6. Acknowledgments

This work was supported by Votorantim Metais Zinc, "FINANCIADORA DE ESTUDOS E PROJETOS – FINEP", and Universidade Federal de Ouro Preto-UFOP. The CNPq and CAPES, scholarship to P. S. Pina and the assistance of José Antônio Magalhães in the experimental work are gratefully acknowledged.

2.7. References

Aydogan, S., Aras, A. and Canbazoglu, M., 2005. Dissolution kinetics of sphalerite in acidic ferric chloride leaching. Chemical Engineering Science, 114: 67-72.

Babu, M.N., Sahu, K.K. and Pandey, B.D., 2002. Zinc recovery from sphalerite concentrate by direct oxidative leaching with ammonium, sodium and potassium persulphates. Hydrometallurgy, 64: 119-129.

Baldwin, S.A., Demopoulos, G.P. and Papangelakis, V.G., 1995. Assessment of alternative iron sources in the pressure leaching of zinc concentrates using reactor model. Hydrometallurgy, 39: 147-162.

Bobeck, G.E. and Su, H., 1985. The kinetics of dissolution of sphalerite in ferric chloride solutions. Metallurgical Transactions B, 16: 413-424.

Crundwell, F.K., 1987. Kinetics and mechanisms of the oxidative dissolution of a zinc sulphide concentrate in ferric sulphate solutions Hydrometallurgy, 19: 227-242.

Crundwell, F.K., 1988. The influence of the electronic structure of solids on the anodic dissolution and leaching of semiconducting sulphide minerals. Hydrometallurgy, 21: 155-190.

Crundwell, F.K. and Verbaan, B., 1987. Kinetics and Mechanisms of the non-oxidative dissolution of sphalerite (zinc sulphide). Hydrometallurgy, 17: 369-384.

Deller, G., 2005. World zinc supply and demand – heading for a late-decade price spike. In: Y. Umetsu (Editor), The Lead & Zinc '05 committees, Kyoto, Japan, pp. 17 - 25.

Dutrizac, J.E., 1992. The leaching of sulphide minerals in chloride media. Hydrometallurgy, 29: 1-45.

Dutrizac, J.E., 2005. The kinetics of sphalerite dissolution in ferric sulphate-sulphuric acid media. In: Y. Umetsu (Editor), The Lead & Zinc '05 committees, Kyoto, Japan, pp. 833-851.

Dutrizac, J.E. and MacDonald, R.J.C., 1978. The dissolution of sphalerite in ferric chloride solution. Metallurgical Transactions B, 09: 543-551.

Garcia, M.A., Mejías, A., Martín, D. and Diaz, G., 2000. Upcoming zinc mine projects: the key for success in zincex solvent extraction. In: J.E. Dutrizac, G.J. A., D.M. Henke, S.E. James and A.H.J. Siegmund (Editors), Lead-Zinc 2000. TMS, Pennsylvania, USA, pp. 751-762.

Ghosh, M.K., Das, R.P. and Biswas, A.K., 2002. Oxidative ammonia leaching of sphalerite Part I: Noncatalytic kinetics. International journal of mineral processing, 66 (241– 254.).

Jin, Z.M., Warren, G.W. and Henein, H., 1984. Reaction-Kinetics of the Ferric-Chloride Leaching of Sphalerite - an Experimental-Study. Metallurgical Transactions B-Process Metallurgy, 15(1): 5-12.

Levenspiel, O., 1999. Chemical reaction engineering. John Wiley & Sons, New York, 664 pp.

Lizama, H.M., Fairweather, M.J., Dai, Z. and Allegretto, T.D., 2003. How does bioleaching start? Hydrometallurgy, 69(109-116).

Madhuchbanda, M., Devi, N.B., Rath, P.C., Kao, K.S. and Paramguru, R.K., 2003. Leaching of manganese nodule in hydrochloric acid and in presence of sphalerite. Can. Metall. Q 42, 49-60. Canadian Metallurgical Quartely, 42: 49-60.

Markus, H., Fugleberg, S., Valtakari, D., Salmi, T., Murzin, D.Y. and Lahtinen, M., 2004. Kinetic Modelling of a solid-liquid reaction: reduction of ferric iron to ferrous iron with zinc sulphide. Chemical Engineering Science, 59: 919-930.

Massaci, P., Recinella, M. and Piga, L., 1998. Factorial experiments for selective leaching of zinc sulphide in ferric sulphate media. International journal of mineral processing, 53 (213– 224).

Palencia Perez, I. and Dutrizac, J.E., 1991. The effect of the iron content of sphalerite on its rate of dissolution in ferric sulphate and ferric chloride media. Hydrometallurgy.

Rath, P.C., Paramguru, R.K. and Jena, P.K., 1988. Kinetics of dissolution of sulphide minerals in ferric chloride solutions, 1: dissolution of galena, sphalerite and chalcopyrite. Transactions Institute of Mining and Metallurgy, 97: 150-158.

Silva, G., 2004. Relative importance of diffusion and reaction control during the bacterial and ferric sulphate leaching of zinc sulphide Hydrometallurgy, 73(313-324).

Souza, A.D., 2005. Processo integrado: biolixiviação e lixiviação química na indústria do zinco. Master Thesis, Federal University of Ouro Preto, Ouro Preto, Brazil, 98 pp.

Souza, A.D., Leão, V.A. and Pina, P.S., 2006. Bioleaching and chemical leaching as an integrated process in the zinc industry. Minerals Engineering. In press

Svens, K., Kerstiens, K. and Runkel, M., 2003. Recent experiences with modern zinc processing technology. Erzmetall, 56: 94-103.

Weisener, C.G. and Smart, R.S.C.G., A. R., 2003. Kinetics and mechanisms of the leaching of low Fe sphalerite Geochimica et Cosmochimica acta, 67: 823-830.

CAPÍTULO 3

A KINETICS STUDY OF THE SULPHURIC ACID LEACHING OF A ZINC SILICATE CALCINE

Abstract

The recent developments of acid-leaching and solvent extraction of zinc silicate ores have produced renewed commercial interest in these ores. Notwithstanding, the leaching kinetics of these concentrates have received little attention so far. This work sought, therefore, to address the leaching of a zinc silicate concentrate in sulphuric acid. The effects of particle size (0.038–0.075 mm), temperature (30–50^{o}C) and initial acid concentration (0.2–1.0 mol/L) were studied. The results show that decreasing the particle size while increasing the temperature and acid concentration increase the leaching rate. As leaching occurs, there is a progressive dissolution of willemite while the quartz and iron-containing phases remain inert. Among the kinetic models of the porous solids tested, the grain model with porous diffusion control successfully described the zinc leaching kinetics. The model enabled the determination of an activation energy of 51.9 ± 2.8 kJ/mol and a reaction order of 0.64 ± 0.12 (with respect to sulphuric acid), which are likely to be a consequence of the parallel nature of diffusion and chemical reaction in porous solids.

Key words: zinc silicate, grain model, diffusion control, willemite.

3.1. Introduction

Non-sulphide zinc deposits are genetically classified into two categories. One is the supergene deposits, derived from zinc sulphides. The other class is formed by the so-called hypogene deposits, recognized as non-sulphide zinc minerals (formed by willemite or a willemite-franklinite-zincite-gahnite association). The recent developments of acid leaching (Votorantim, Brazil) and solvent extraction (Tecnicas Reunidas, Spain) of zinc silicate concentrates have produced renewed commercial interest in these ores. Within the foreseeable future, the annual production of zinc from non-sulphide sources could vastly exceed 10% of global metal production (Boni, 2005). Accordingly, Votorantim Metais Zinc (VMZ) has devised an integrated process to treat both zinc sulphides and silicates (Souza et al., 2007). The process consists of the leaching of zinc silicate ores (willemite, Zn_2SiO_4, and hemimorphite, $Zn_4Si_2O_7(OH)_2.H_2O$), in the same plant that treats zinc sulphide concentrates through the traditional RLE (roasting-leaching-electrolysis) process.

In the integrated process (Souza, 2000), as calcium and magnesium carbonates are present in the zinc concentrate, this concentrate is treated with zinc wash solution (about 45g/L of zinc) to obtain a slurry. This slurry is submitted afterwards to a step where zinc is precipitated as basic zinc sulphate ($ZnSO_4.3Zn(OH)_2.4H_2O$, (Chen and Dutrizac, 2003)) while the magnesium remains in the solution as its respective sulphate (equation 3.1).

$$3ZnSO_4 + 0.5Zn_2SiO_4 + 7H_2O + CaCO_3 + MgCO_3 \rightarrow ZnSO_4.3Zn(OH)_2.4H_2O + 0.5SiO_2 + CaSO_4 + MgSO_4 + 2CO_2 \quad (3.1)$$

Zinc is precipitated at 95ºC or alternatively, at 180-200ºC and 18 bar pressure, so that basic zinc sulphate is readily formed (Souza, 2000). The influent wash solution pH is 5.0 and reaches pH 6.6 after neutralization by the carbonates, present in the silicate concentrate, which results in zinc precipitation from the wash solution. The basic zinc sulphate is dissolved afterwards with a 180g/L sulphuric acid solution, which has been returned from the electrolysis step (spent solution) of the RLE process. After thickening and filtration, the clarified solution is sent to the neutral leaching (pH 4.0) step of the RLE process, completing the integration of the sulphide and non-sulphide concentrate treatment (Souza, 2000).

Direct silicate leaching with sulphuric acid can be represented by equations (3.2) and (3.3) for hemimorphite and willemite, respectively.

$$Zn_4Si_2O_7(OH)_2.H_2O + 4H_2SO_4 \rightarrow 4ZnSO_4 + Si_2O(OH)_6 + 3H_2O \quad (3.2)$$

$$Zn_2SiO_4 + 2H_2SO_4 \rightarrow 2ZnSO_4 + Si(OH)_4 \quad (3.3)$$

The monosilic acid ($Si(OH)_4$), produced in equation (3.3), polymerizes and may form particles of colloidal silica (Espiari et al., 2006). Besides, a gel is formed which is not filterable. Much effort has been applied to precipitate silica without forming the latter. Some authors have suggested the use of flocculants, as aluminium sulphate, to remove the silica gel while others have proposed the use of microwave radiation for the same purpose (Hua et al., 2002).

The kinetics of zinc silicate dissolution is far less studied than that of zinc sulphides. Terry and Monhemius (1983) have comprehensively studied the leaching kinetics of

natural hemimorphite, as well as natural and synthetic willemite. The authors have observed that the acidic dissolution was diffusion-controlled for hemimorphite and chemically-controlled for willemite leaching. Abdel-Aal (2000), studying the leaching kinetics of low grade zinc silicate, proposed that the process was controlled by diffusion on an "ash" layer with an associated activation energy of 13.4 kJ/mol (3.2 kcal/mol). As shown in equations (3.2) and (3.3), there is no solid reaction product formed during leaching, as only zinc ions and silica gel are produced, although the latter can affect the transport properties of the solution. It should be pointed out that Abdel-Aal (2000) did not present an explanation for the proposed diffusion control in the product layer. It is also possible that diffusion through the solid's pores would explain the controls observed during silicate leaching. It has been shown that if the transport through a solid's pores is the rate-determining step, an expression similar to the shrinking core model (SCM) with diffusion control (Georgiou and Papangelakis, 1998) is achieved.

This work addresses the leaching kinetics of a zinc silicate calcine which can be represented by a variant of the SCM when diffusion through the product layer is the rate-determining step.

3.2. Materials and Methods

The zinc silicate calcine, assaying 43.5% Zn (table 1), was produced by roasting a zinc silicate floatation concentrate in a rotatory kiln at temperatures of 700-800^{o}C, for 60 minutes aiming at removing organic matter. XRD of the calcine showed the presence of willemite (Zn_2SiO_4) as the main zinc-containing phase and franklinite ($ZnO.Fe_2O_3$) as a

minor constituent. This was based on the iron content of the zinc silicate calcine (table 3.2). Hematite and magnetite as well as quartz and dolomite constituted the gangue.

Table 3.1. Chemical analysis of the bulk zinc silicate calcine.

%Zn	%SiO_2	%Fe	%Cd	%Cu	%Co	%Pb
43.50	23.30	5.90	0.01	0.003	0.003	1.25

Table 3.2. Chemical analysis (Zn and Fe) and surface area of different screened fractions of the zinc silicate calcine.

Size fraction	% Zn	% Fe	Surface area (m^2/g)	Total pore volume (mm^3/g)	Pore average diameter (nm)
105-75µm	44.50	3.64	2.0	8.8	17.2
75-53µm	46.44	3.59	2.6	8.8	13.6
53-45µm	45.51	4.53	2.3	11.8	20.3
45-38µm	44.48	4.48	2.5	12.9	20.7

Prior to the leaching experiments, the zinc calcine was dry-ground and wet-sieved to yield a particle size distribution between 150 µm and 38 µm. The zinc and iron content as well as surface area, total porous volume and porous average diameter of the different sieved fractions are also depicted in table 3.2. The chemical leaching tests were carried out batchwise in a closed water-jacket borosilicate glass reactor with 750 mL total volume, and agitation was provided by a magnetic stirrer. That enabled adequate dispersion of the mineral particles without evaporation loss of the solution. The leaching temperature was evaluated in the range of 30 to 60^oC and the acid

concentration between 0.2 and 1.0 mol/L was studied. The solution volume was 500 mL and the solid concentration, 10 g/L. Leaching solutions were prepared using reagent grade chemicals (H_2SO_4, *Synth*) and distilled water. At selected time intervals, a known amount (3 mL) of slurry was withdrawn and filtered. The first sample was taken after 30 seconds of contact between the solid and solution, and 10 seconds was required for each sampling and filtration procedure. The zinc extraction was determined by analyzing zinc concentration in solution (Atomic Absorption Spectrometry, Perkin Elmer AAnalyst 100) and for every sample taken from the reactor, the volume change was taken into account in the zinc extraction determinations, which were calculated based on the mass of zinc dissolved as function of time, according to the following equation:

$$Zn.extr = \frac{[Zn]_{T0+T}}{[Zn]_{T0}}.100 \qquad (3.4)$$

Surface area and pore volume were determined by nitrogen adsorption. Nitrogen isotherms were performed with a Nova 1000 High Speed Gas Sorption Analyzer (*Quantachrome*). Sample degassing was carried out at 80°C, for 24 hours, to avoid decomposition. Nitrogen adsorption was performed at -196°C. Data were collected from a relative pressure (p/p_0) of 0.05 to 0.98. A large sample (~4.0g) was used and the Nova 1000 parameters (equilibration tolerance, time to remain in tolerance and maximum equilibration time) were set at 0.05, 360 and 720, respectively, to improve the accuracy of low surface area measurements with nitrogen adsorption.

The analyses of the silicate calcine and leaching residues were carried out by SEM-EDS. The samples were coated with graphite by electro-deposition, using a Jeol JEE 4C

instrument and observed in a JEOL JSM 5510 scanning electron microscope (SEM), equipped with a spectrometer for micro-analysis based on a Energy dispersive x-ray spectroscopy system (EDS), and having an accelerating voltage 0.5-30kV. Electron microprobe analysis have confirmed willemite as the main zinc mineral since the metal content of different grains is similar to that of a pure mineral (theoretical, table 3.3).

Table 3.3. EDS analysis (Zn, Si and O) of the zinc silicate calcine (average of 6 points).

Element	EDS analysis	Pure Willemite
Zn	49.52	32.57
Si	49.46	32.28
O	48.13	32.63

Statistical analysis was carried out using the Origin™ version 6.0 software which determined both the activation energies and the order of reactions with respect to sulphuric acid determined for a 95% confidence interval.

3.3. Results and discussion

3.3.1. Effect of agitation speed

Figure 3.1 shows the effect of the stirring speed on zinc dissolution. The increase of the stirring speed in the range 360 - 720 rpm does not increase zinc extraction. Therefore, the dissolution process does not seem to be controlled by mass transfer through the liquid boundary layer, despite the change in solution viscosity caused by the formation of silica gel. As a result, the stirring speed was kept at 480rpm, unless otherwise stated.

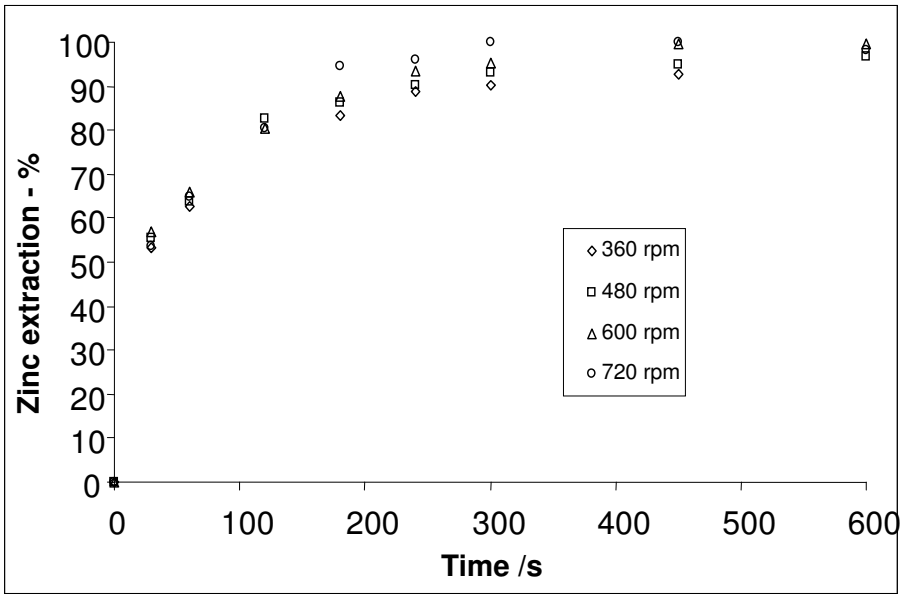

Figure 3.1. Effect of stirring rate on zinc extraction. 0.4 mol/L H_2SO_4, 10 g/L solids, temperature 40 ºC and particle size 75-53 μm.

3.3.2. Effect of the temperature

Figure 3.2 shows the change of zinc extraction with time as a function of temperature in the range of 30 – 60ºC. The zinc extraction increases with the leaching temperature,

implying that temperature has an important role in the zinc dissolution process. Similar results were observed by Bodas (1996) and Espiari et al. (2006), that carried out leaching experiments with a zinc silicate ore containing hemimorphite ($Zn_4Si_2O_7(OH)_2.H_2O$) and smithsonite ($ZnCO_3$) as major zinc minerals. Similarly, Abdel-Aal (2000) studied the leaching of a zinc silicate ore containing willemite and hemimorphite and observed that as temperature was increased from 40 °C to 70 °C, zinc extraction enhanced from 70 to 95%.

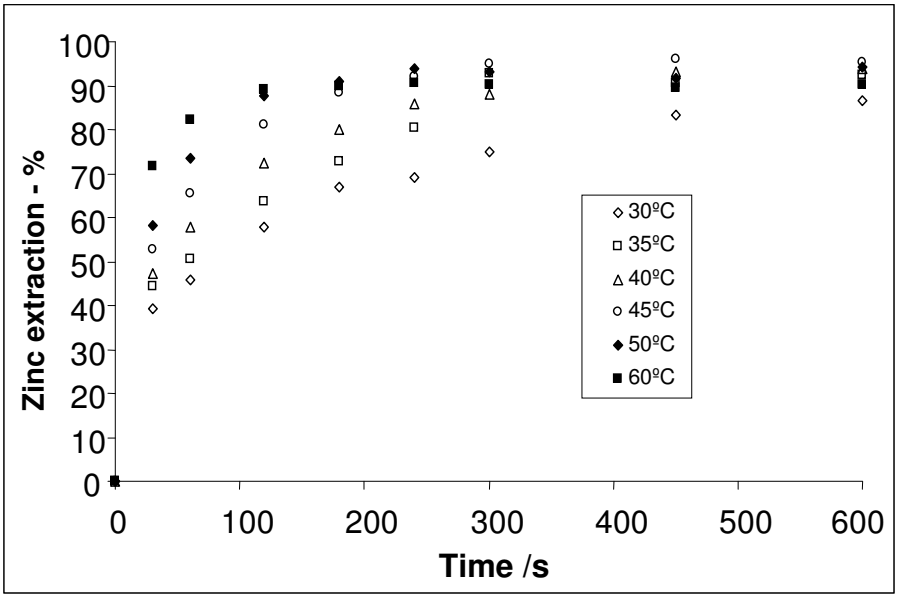

Figure 3.2. Effect of temperature on zinc extraction. 0.4 mol/L H_2SO_4, 10 g/L solids, stirring rate 480 rpm and particle size 75-53 μm.

3.3.3. Effect of the sulphuric acid concentration

Figure 3.3 presents the effect of the sulphuric acid concentration on zinc extraction as a function of time. The zinc extraction rate increases with the sulphuric acid concentration, in the range being assessed in this study. This behaviour was observed in previous works, carried out by Bodas (1996), Abdel-Aal (2000) and Espiari et al.

(2006), in experiments performed in a sulphuric acid medium. Terry and Monhemius (1983) studied the effect of sulphuric, nitric, phosphoric and hydrochloric acid concentrations upon zinc dissolution from natural willemite samples. The authors observed that the zinc dissolution rate was strongly dependent on both acid concentration (the increase in the proton concentration enhanced the zinc dissolution rate) and the acidic anion (SO_4^{2-}, PO_4^{3-}, Cl^- and NO_3^-). The following reactivity order was observed by the authors with respect to the acidic anion: $HCl \approx HNO_3 < HClO_4 < H_2SO_4 \approx H_3PO_4$. Terry and Monhemius (1983) suggested that the difference in the reactivity order was in function of the complex affinity for the zinc ion.

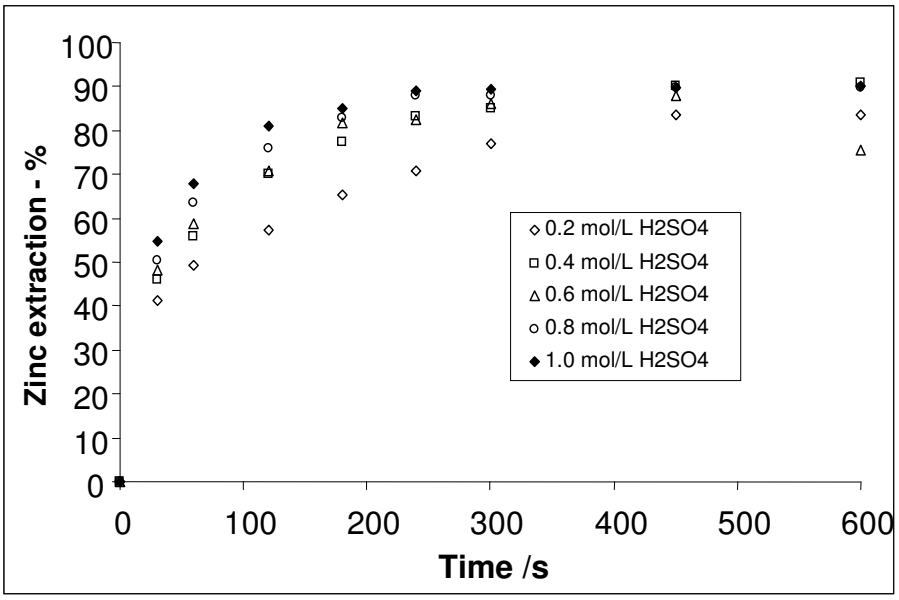

Figure 3.3. Effect of acid concentration on zinc extraction. Stirring rate 480 rpm, 10 g/L solids, temperature 40 ºC and particle size 75-53µm.

3.3.4. Effect of the particle size

The decrease in particle size enhanced zinc dissolution (figure 3.4), although the zinc extraction observed in the experiment carried out, with the particle size between 38 -45

µm, is only 7% higher than that obtained in the experiment carried out in the 75 – 53 µm range. The small difference observed can be likely ascribed to the negligible increasing of the particle surface area (BET surface area) with decreasing particle sizes as an effect of the porosity of the solid (table 3.2). Massaci et al. (1998) also observed the insignificance of particle size on the leaching kinetics, while they were studying a zinc sulphide ore leaching in ferric sulphate media. The authors credited this behaviour to the presence of a natural porosity in the zinc sulphide particles, but they did not present surface area and porosity analysis. Usually, the literature shows that the smaller the particle size, the faster the reaction rate, as observed by Abdel-Aal (2000). The high reactivity of the roasted silicate in sulphuric acid medium associated to a small difference in the surface area of the different size fractions, could have masked the effect of particle size upon the zinc leaching rate (Aydogan et al., 2005; Bobeck and Su, 1985; Ghosh et al., 2002; Silva, 2004).

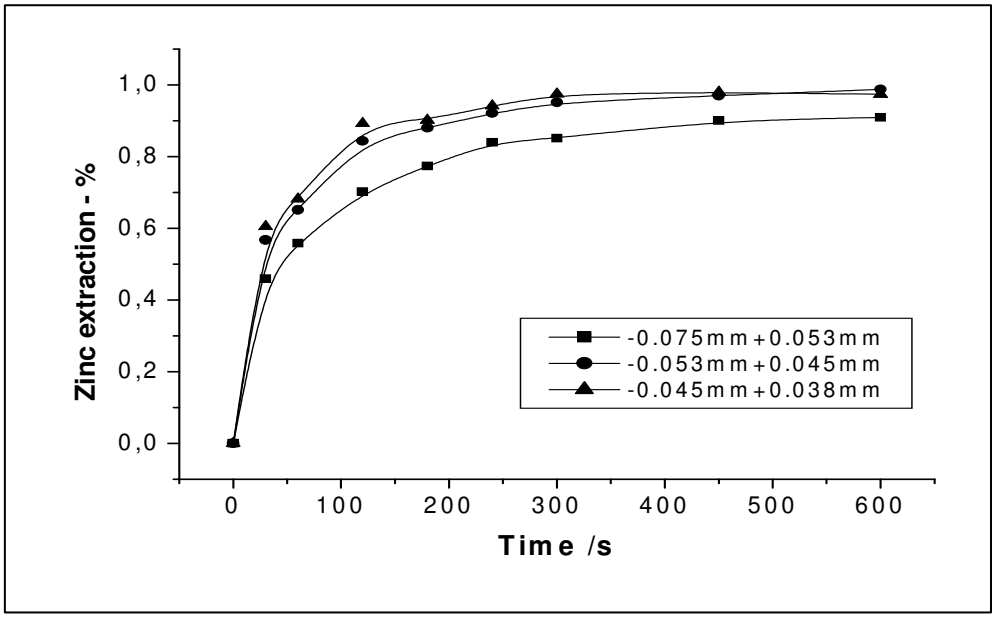

Figure 3.4. Effect of particle size on zinc extraction. Stirring rate 480 rpm, 10 g/L solids, temperature 40 ºC and 0.4 mol/L H_2SO_4.

3.3.5. Morphology of the leaching residues

The morphology of the zinc silicate calcine particles before and after leaching was examined by SEM-EDS. The solid particles present a rough and porous surface generated by the calcination process that resulted in the sintering of the small particles found on the surface of the larger ones, as observed in the figures 3.5(a) and (b). The micrograph of the leaching residues shows a progressive increase in the roughness and porosity of the solid. For instance, after 45% zinc extraction (figures 3.5(c) and (d)), the particles present a high degree of degradation, that sharply increases along the progress of dissolution (figure 3.5(e) and (f)). In spite of the surface degradation generated by the leaching process, figures 3.5(a-f) suggest that the particle surface does not present a reaction product layer. Notwithstanding, as shown in the XRD patterns (figure 3.6) of the zinc silicate and the leaching residues (after 1 and 3 minutes), willemite is selectively leached, while the quartz and iron-containing phases (hematite and magnetite) remain as an "ash" layer. Therefore, it is proposed that the zinc dissolution process be controlled by diffusion of the reagent in the porous structure of the calcine particles, as observed by (Georgiou and Papangelakis, 1998) in pressure leaching experiments carried out with limonitic laterite ores.

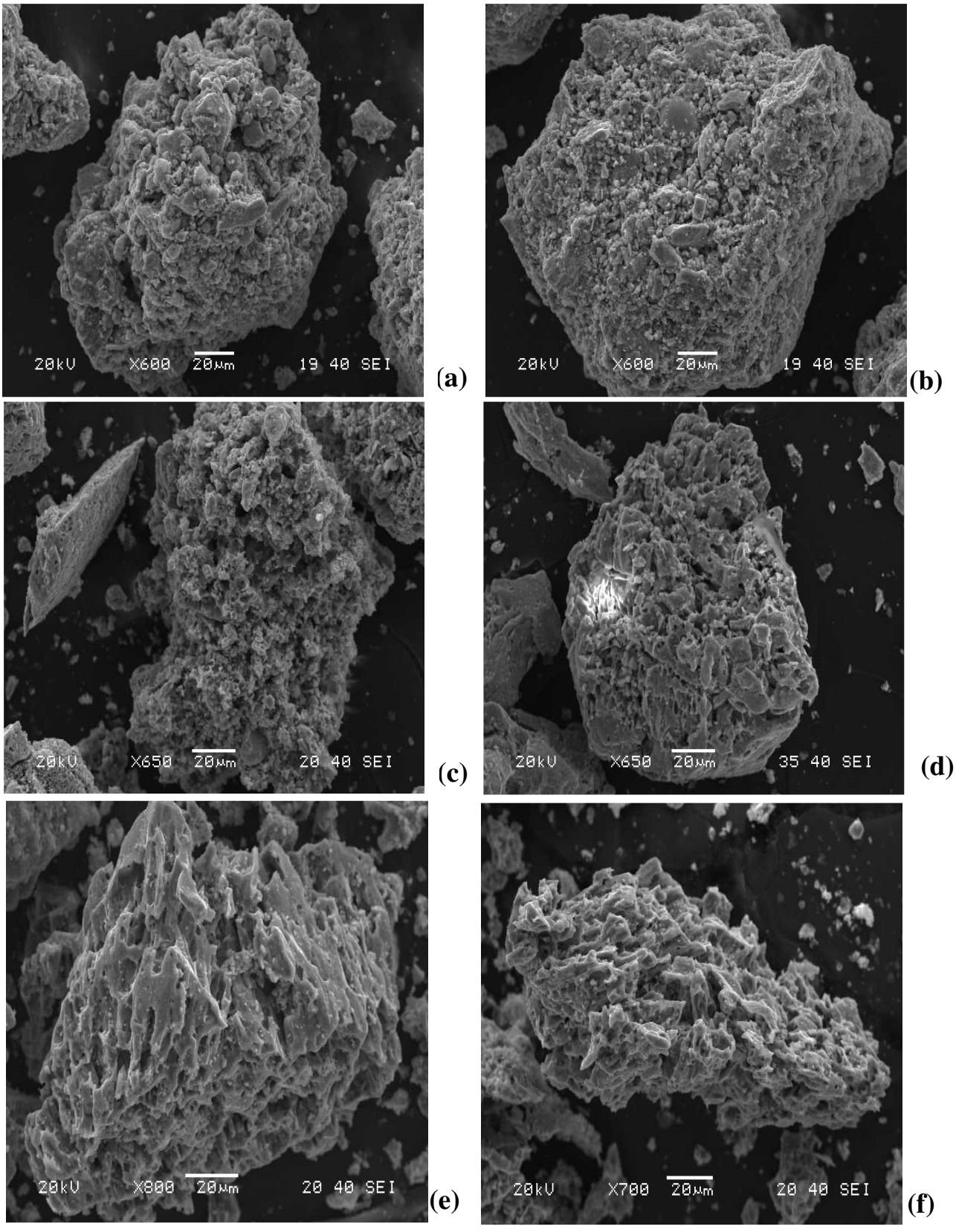

Figure 3.5. Particles of zinc silicate calcine before leaching (a and b); after 45% zinc extraction (c and d) and after 80% zinc extraction (e and f). Particle size range 105-150µm.

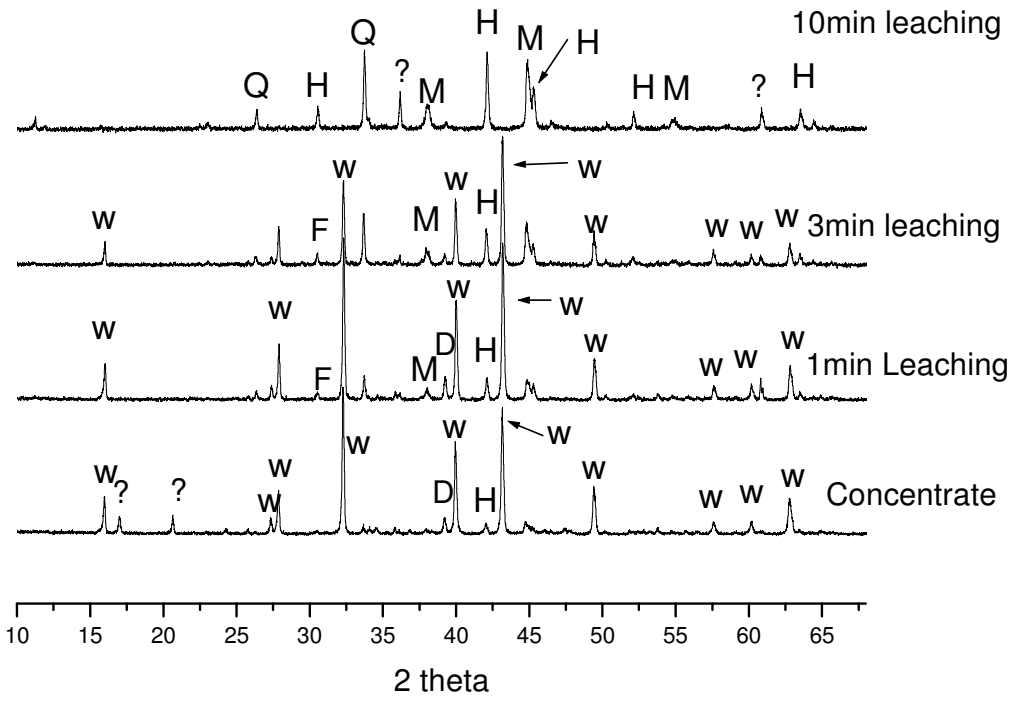

Figure 3.6. XRD pattern of the zinc silicate calcine. Q: quartz, H: hematite, M: magnetite, W: willemite, F: Franklinite, D: dolomite.

3.3.6. Kinetics analysis

The leaching of zinc silicate calcine in sulphuric acid solutions includes a heterogeneous reaction as represented by equations 3.2 and 3.3. Assuming that the zinc silicate particles have a spherical geometry and the chemical reaction is the rate-controlling step, the following expression of the shrinking core model can be tested to describe the dissolution kinetics of the process:

$$1-(1-\alpha)^{\frac{1}{3}} = k_R.t\,, \quad k_R = \frac{b.k.[H_2SO_4]^n}{\rho_{silicate}.r_o} \tag{3.5}$$

Similarly, when the diffusion of the reagent through a product layer is the rate-controlling step, the following expression of the shrinking core model is achieved to describe the dissolution kinetics:

$$1-3(1-\alpha)^{\frac{2}{3}}+2(1-\alpha)=k_d.t \text{, where } k_d=\frac{6.b.D_{eff}.[H_2SO_4]}{\rho_{silicate}.r_o^2} \quad (3.6)$$

According to equations 3.5 and 3.6, when chemical reaction is the rate-controlling step, a plot of $[1-(1-\alpha)^{1/3}]$ versus time is a straight line with a slope k_R. Conversely, when the process is controlled by diffusion through the solid product layer, a plot of $[1-3(1-\alpha)^{2/3}+2(1-\alpha)]$ versus time is also a straight line whose slope is k_d (Levenspiel, 1999). Furthermore, for all purposes, k can be written as $k = A.k_0.[H_2SO_4]^n$ where A stands for area of reaction; k_0 for the Arrhenius pre-exponential factor; $[H_2SO_4]$ for acid concentration and n for reaction order.

Figure 3.7 presents the fitting of the SCM model with chemical reaction control (equation 3.5) and product diffusion control (equation 3.6) to the experimental data. It is readily noticed that the model for product diffusion control depicted a better outcome as compared to the one for chemical reaction control. Nevertheless, the dissolution of the zinc silicate calcine occurs without the formation of a product layer, as shown in figure 3.5. Therefore, this model is not consistent with the physical picture of the process, despite the mathematical fitting of the experimental data to the SCM equation for product diffusion control. Thus, equation 3.6 is unlikely to physically represent the reacting system and a different model, which takes into account the effect of porosity, should be tested so that the zinc silicate leaching can be adequately described. In the

latter, the aqueous reactant diffuses and reacts concomitantly so that diffusion and chemical reaction occurs in parallel, instead of in series, as predicted by the shrinking core model applied to non-porous solids (Sohn and Wadsworth, 1979).

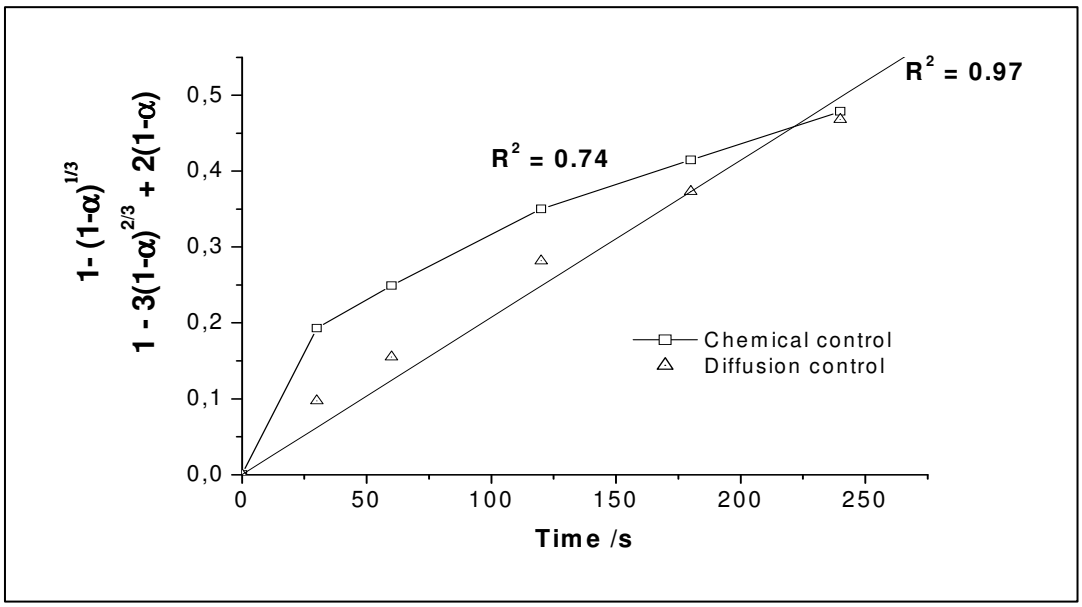

Figure 3.7. Fitting of the shrinking core and grain models. Temperature 40 ºC, 0.4 mol/L H_2SO_4, 10 g/L solids, stirring rate 480 rpm and particle size 75-53 μm.

Several models have been proposed to describe the leaching kinetics of porous solids, such as: (i) the *random pore model*, (ii) the *uniform pore model* and (iii) *the grain model*. The random pore model could not be applied to represent the leaching process as observed elsewhere (Filippou et al., 1997). The uniform pore model with chemical control was also tested to describe the leaching kinetics, but did not produce a good fit to the experimental data, as observed in other hydrometallurgical systems (Filippou et al., 1997; Raghavan and Gajam, 1986). The grain pore model will be discussed further on.

Modelling porous solids leaching kinetics, Sohn and Wadsworth (1979) stated that the concentration of the reactant is uniform throughout the solid when the resistance

associated to diffusion is small. If the diffusion resistance is large, conversely, the reaction occurs in a narrow layer near the external surface because the reactant cannot penetrate deeply inside the pores before reacting. Assuming that external mass transfer is fast and that this layer is much thinner than the particle dimensions, the authors proposed the following equation for the overall rate (r_i):

$$r_i = \left(\frac{2}{n+1} k S_v D_{eff} \right)^{\frac{1}{2}} [i]_s^{\frac{n+1}{2}} \tag{3.7}$$

In equation 3.7, k is the chemical rate constant, and therefore the overall rate is increased even when k is large (the reaction is fast), which means that diffusion alone does not control the overall rate, a consequence of the parallel nature of the chemical reaction and diffusion in porous solids (Sohn and Wadsworth, 1979). An important outcome of equation 3.7 is that both the activation energy and reaction order of the process are an average of the values associated with the chemical reaction and diffusion steps.

The grain model (Szekely et al., 1976) can also be applied to describe the leaching kinetics of porous solids. It considers that the solid reactant is made up of a large number of individual grains of the same size and form, which are similar to the exterior form of the particle (i.e. a spherical particle is formed by spherical non-porous grains). When the reaction is chemically controlled, there is no resistance for diffusion throughout the pores, the fluid reactant concentration is uniform in the whole solid, and an expression similar to equation 3.5 is produced. Nevertheless, if chemical reaction resistance is negligible, as compared to that due to pore diffusion, the reaction occurs in a narrow region and this situation is similar to the shrinking core model with ash layer

control, applied to nonporous solids. The model gives the following expression for spherical particles (Georgiou and Papangelakis, 1998):

$$1-3(1-\alpha)^{\frac{2}{3}}+2(1-\alpha)=\frac{t^{*}}{\hat{\sigma}^{2}} \tag{3.8}$$

being t^{*} and $\hat{\sigma}$ defined as follow:

$$t^{*}=\left(\frac{bk[H_2SO_4]}{4r_0\rho_{silicate}}\right)t \tag{3.9}$$

$$\hat{\sigma}=\frac{r_0}{3}\left(\frac{3k(1-\varepsilon_0)}{8r_0D_{eff}}\right)^{\frac{1}{2}} \tag{3.10}$$

By applying equations (3.9) and (3.10) to solve equation (3.8), the following expression is achieved to describe the zinc silicate leaching:

$$1-3(1-\alpha)^{\frac{2}{3}}+2(1-\alpha)=k_D t \qquad \text{where} \quad k_D=\frac{3bD_{eff}[H_2SO_4]^n}{r_0^2\rho_{silicate}(1-\varepsilon_0)} \tag{3.11}$$

As shown in figure 3.7, a good fit ($r^2 > 0.97$) is observed when the left hand of equation 3.11 is applied to the experimental data. Furthermore, from the analysis of equation 3.11, there is a clear dependence of the model constant, k_D, with the inverse square of initial particle radius ($1/r_0^2$). Figure 3.8 presents the plot of k_D versus $1/r_0^2$ that was obtained from the linear fitting of the data present in the figure 3.4 into equation 3.11. It can be seen from figure 3.8 that there is a linear relationship between the rate constant and the square of the inverse of the initial particle radius, $1/r_0^2$. This behaviour supports

the application of the grain model with pore diffusion control to describe the dissolution kinetics of the zinc silicate calcine.

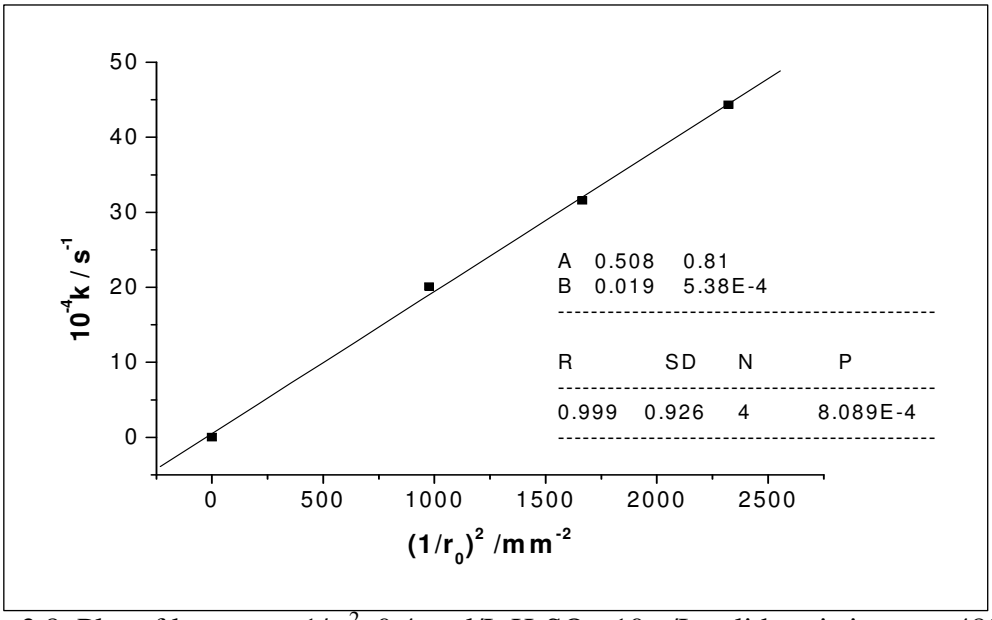

Figure 3.8. Plot of k_D versus $1/r_0^2$. 0.4 mol/L H_2SO_4, 10 g/L solids, stirring rate 480 rpm and 40 ºC. In the estimated linear regression model, A and B represent the values of the intercept and slope, respectively, followed by their respective standard errors. R is the correlation coefficient; N, the number of data points and SD, the standard deviation of the fit.

Figures 3.9 presents the Arrhenius plot constructed with the rate constant value, k_D, calculated from data presented in figure 3.2. The activation energy determined for the pore diffusion control is 51.9 ± 2.8 kJ/mol (12.4 ± 0.7 kcal/mol). This value is similar to those obtained by Terry and Monhemius (1983), that found 49.2kJ/mol (11.8kcal/mol) and 39.0kJ/mol (9.3kcal/mol) for the dissolution of natural and synthetic willemite samples in sulphuric acid solution (pH 1.90), respectively. Similarly, Espiari et al. (2006) found an activation energy of 23.5kJ/mol (5.6kcal/mol) for the dissolution of zinc-rich tailings (smithsonite and hemimorphite) in sulphuric acid solutions and stated that the dissolution process was controlled by an adsorption/desorption process.

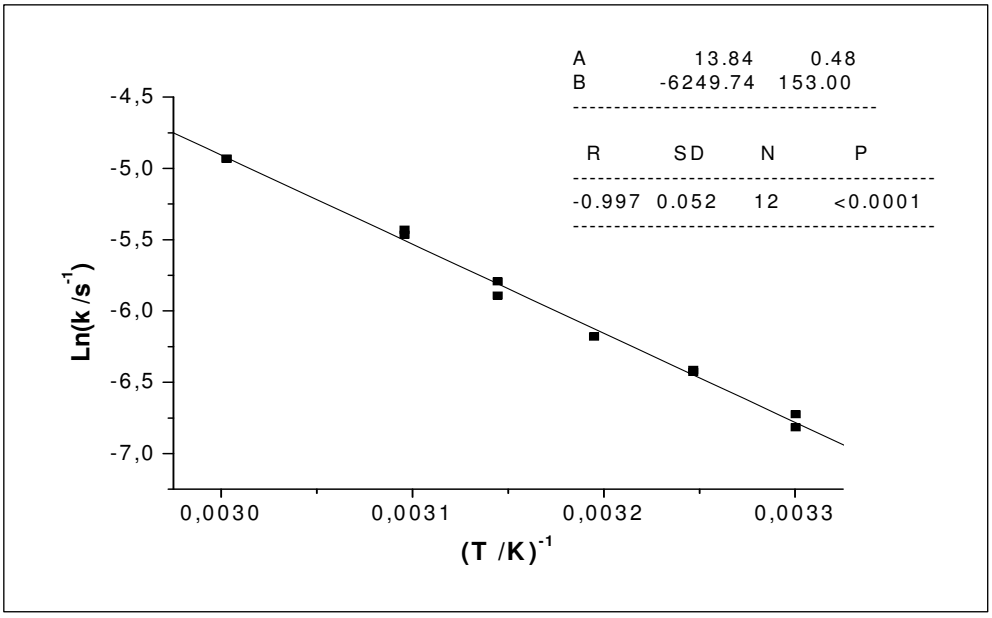

Figure 3.9. Arrhenius plot for the grain model. 0.4 mol/L H_2SO_4, 10 g/L solids, stirring rate 480 rpm and particle size 75-53 μm. In the estimated linear regression model, A and B represent the values of the intercept and slope, respectively, followed by their respective standard errors. R is the correlation coefficient; N, the number of data points and SD, the standard deviation of the fit.

The activation energy determined in the present work is high for the diffusion of ions in solution, although similar values were proposed for the diffusion-controlled leaching of other porous materials, as shown in table 3.4. These values are likely derived from the parallel nature of diffusion and reaction in porous solids as shown in equation 3.7. This implies that the apparent activation energy is the average of that for intrinsic reaction and diffusion, as already stated. Nevertheless, when the zinc silicate leaching is diffusion controlled, the effective diffusion coefficient, determined from equation 3.11, should be smaller than that for aqueous solutions. Table 3.5 presents the values for the effective diffusion coefficients of sulphuric acid as a function of the leaching temperature (from 30ºC to 60ºC). The effective diffusion coefficient slightly increases with temperature, in the range studied in this work, as expected. Nizikou et al. (1997) determined the diffusion coefficient of sulphuric acid in higher than 0.2mol/L aqueous

solutions and 25°C. According to the authors, a value of 1.8 x 10^{-5} cm^2/s (25°C) is proposed for the diffusion of sulphuric acid in aqueous solutions, which is the same as that calculated using the equations proposed by Umino and Newman (1997), considering that their model can be applied to a 0.4 mol/L solution. Utilizing the activation energy determined in the present work, a diffusion coefficient of $1.2x10^{-7}$ cm^2/s was estimated at 25°C for the zinc silicate leaching, which is two orders of magnitude lower than that proposed for aqueous solutions. Similarly, the apparent reaction order, with respect to sulphuric acid, determined from figure 3.3, as 0.64 ± 0.12 (figure 3.10) is also an average for the chemical reaction and diffusion values (Sohn and Wadsworth, 1979). Summarizing, the leaching of zinc silicate is likely controlled by the transport inside the silicate pores.

Table 3.4. Selected values of activation energies observed during the leaching of porous materials.

Material being leached	Experimental conditions	Activation energy (kJ/mol)	Reference
Spent nickel catalyst	10% solids, 50-90°C, sulfuric acid	69.1	(Sahu et al., 2005)
Chalcopyrite leaching with $Na_2Cr_2O_7$	Stoichiometric amount of reactant-molybdenite concentrate	40	(Ruiz and Padilla, 1998)
Leaching of Ni smelter slag	Leaching in the presence of SO_2, 4-35°C, 1% solids, 600rpm	70 (for Co, Fe)50 (for Ni)	(Gbor et al., 2000)
Niobium leaching with NaOH	30% solids, 300g/L KOH, 150-200°C, Nb concentrate	72.2	(Zhou et al., 2005)
Acid pressure leaching of Limonite	30% solids, 230-150°C, 64.8m^2/g surface area, H_2SO_4/ore ratio: 0.2	85.4 (estimated)	(Georgiou and Papangelakis, 1998)

Table 3.5. Effective diffusion coefficients of H_2SO_4 as a function of temperature (0.4 mol/L H_2SO_4, 10g/L solids (w/v), stirring rate 480 rpm and particle size 75-53μm).

Temperature (°C)	D_{eff} (cm^2/s)
30	$1.7x10^{-7}$
35	$2.4x10^{-7}$
40	$3.1x10^{-7}$
45	$4.3x10^{-7}$
50	$6.3x10^{-7}$
60	$10.6\ x10^{-7}$

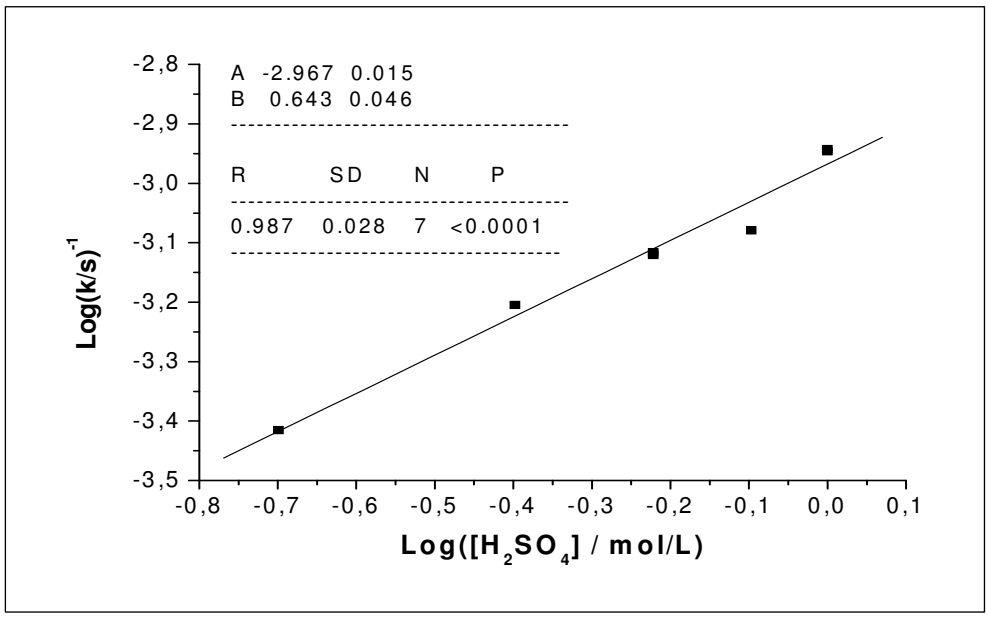

Figure 3.10. Plot of k_D as a function of the sulphuric acid concentration. 40 °C, 10 g/L solids, stirring rate 480 rpm and particle size 75-53 μm. In the estimated linear regression model, A and B represent the values of the intercept and slope, respectively, followed by their respective standard errors. R is the correlation coefficient; N, the number of data points and SD, the standard deviation of the fit.

The results of the present work suggest that the zinc silicate leaching is not strongly affected by the particle size, implying that fine grinding of such concentrates is not required. Therefore, a rigid control of the size reducing process is not necessary and the energy consumption during grinding could be reduced. Finally, as diffusion inside the pores is the as the slowest step, it is likely that an increase in the stirring speed could only marginally affect the leaching rate, as the diffusion inside the pores is not strongly affected by stirring in the bulk. Except for the practical effect of solids settling inside the reactors, a complex and expensive stirring system is not required.

3.4. Conclusions

The dissolution kinetics of a roasted zinc silicate (willemite) concentrate in sulphuric acid solutions was studied. It was found that the zinc extraction was fast and increased with temperature and sulphuric acid concentration. The shrinking core model with diffusion control fitted the experimental results, although it could not physically represent the leaching kinetics. The use of the grain model, which successfully described the dissolution of zinc analysis of the zinc silicate particles, is suggested because there was no reaction product on the particle surfaces. The apparent activation energy and reaction order were determined as 51.9 ± 2.8 kJ/mol and 0.64 ± 0.12, respectively, in consequence of the parallel nature of the chemical reaction and diffusion in porous solids.

3.5. Acknowledgments

This work was supported by Votorantim Metais Zinc, "FINANCIADORA DE ESTUDOS E PROJETOS – FINEP", and Universidade Federal de Ouro Preto-UFOP. The CAPES scholarship to P. S. Pina and the assistance of Mr. J. A. Magalhães and Ms. H. K. Reis, are gratefully acknowledged.

3.6. Notation

[i]	Molar concentration of species i
$[i]_s$	Molar concentration of species i at the outer surface of the particle
A	Surface area
B	Stoichiometric coefficient
D_{eff}	Effective diffusion coefficient
K	Chemical rate constant
k_0	Arrhenius pre exponential factor
k_d	Apparent diffusion rate constant for non porous particles
k_D	Apparent diffusion rate constant according to the grain model
k_R	Apparent chemical reaction rate constant for non porous particles
N	Reaction order
r_i	Rate of reaction of species i
r_0	Initial particle radius
S_v	Surface area per unit volume
T	Time
t^*	Grain model parameter

$Zn.extr$ Zinc extraction (%)

$[Zn]_{T0}$ Initial zinc mass (g)

$[Zn]_{T0+T}$ Solids zinc content (g) at T_{0+T}

Greek letters

α Conversion

$\rho_{silicate}$ Silicate molar density

Σ Particle size parameter, dimensionless, see equation 8.

ε_0 Initial porosity of the solid (total pore volume (table 2) x silicate density ($4.0 g/cm^3$))

3.7. References

Abdel-Aal, E.A., 2000. Kinetics of sulphuric acid leaching of low-grade zinc silicate ore. Hydrometallurgy, 55(3): 247-254.

Aydogan, S., Aras, A. and Canbazoglu, M., 2005. Dissolution kinetics of sphalerite in acidic ferric chloride leaching. Chemical Engineering Science, 114: 67-72.

Bobeck, G.E. and Su, H., 1985. The kinetics of dissolution of sphalerite in ferric chloride solutions. Metallurgical Transactions B, 16: 413-424.

Bodas, M.G., 1996. Hydrometallurgical treatment of zinc silicate ore from Thailand. Hydrometallurgy, 40(1-2): 37-49.

Boni, M. 2005. The geology and mineralogy of non-sulphide zinc ore deposits. In: Lead & Zinc '05. Y. Umetsu (ed.) Kyoto, Japan, TMS, Warrendale, PA. pp. 1299-1313.

Chen, T. and Dutrizac, J., 2003. Filter press plugging in zinc plant purification circuits. JOM Journal of the Minerals, Metals and Materials Society, 55(4): 28-31.

Espiari, S., Rashchi, F. and Sadrnezhad, S.K., 2006. Hydrometallurgical treatment of tailings with high zinc content. Hydrometallurgy, 82(1-2): 54-62.

Filippou, D., Konduru, R. and Demopoulos, G.P., 1997. A kinetic study on the acid pressure leaching of pyrrhotite. Hydrometallurgy, 47(1): 1-18.

Gbor, P.K., Ahmed, I.B. and Jia, C.Q., 2000. Behaviour of Co and Ni during aqueous sulphur dioxide leaching of nickel smelter slag. Hydrometallurgy, 57(1): 13-22.

Georgiou, D. and Papangelakis, V.G., 1998. Sulphuric acid pressure leaching of a limonitic laterite: chemistry and kinetics. Hydrometallurgy, 49(1-2): 23-46.

Ghosh, M.K., Das, R.P. and Biswas, A.K., 2002. Oxidative ammonia leaching of sphalerite Part I: Noncatalytic kinetics. International Journal of Mineral Processing, 66 241-254.

Hua, Y., Lin, Z. and Yan, Z., 2002. Application of microwave irradiation to quick leach of zinc silicate ore. Minerals Engineering, 15(6): 451-456.

Levenspiel, O., 1999. Chemical reaction engineering. John Wiley & Sons, New York, 664 pp.

Massaci, P., Recinella, M. and Piga, L., 1998. Factorial experiments for selective leaching of zinc sulphide in ferric sulphate media. International Journal of Mineral Processing, 53 213-224.

Nzikou, J.M., Baklouti, M., Vincent, L.-M. and Lapicque, F., 1997. Improvement in the measurement of diffusion coefficients in a restricted diffusion cell: Case of binary electrolytes. Chemical Engineering and Processing, 36(2): 161-165.

Raghavan, S. and Gajam, S.Y., 1986. Application of an enlarging pore model for the ammoniacal leaching of chrysocolla. Hydrometallurgy, 16(3): 271-281.

Ruiz, M.C. and Padilla, R., 1998. Copper removal from molybdenite concentrate by sodium dichromate leaching. Hydrometallurgy, 48(3): 313-325.

Sahu, K.K., Agarwal, A. and Pandey, B.D., 2005. Nickel recovery from spent nickel catalyst. Waste Management & Research, 23: 148-154.

Silva, G., 2004. Relative importance of diffusion and reaction control during the bacterial and ferric sulphate leaching of zinc sulphide. Hydrometallurgy, 73: 313-324.

Sohn, H.Y. and Wadsworth, M.E., 1979. Rate processes of extractive metallurgy. Plenum Press, New York, 472 pp.

Souza, A.D., 2000. Integration process of the treatments of concentrates or zinc silicates ore and roasted concentrate of zinc sulphides.

Souza, A.D., Pina, P.S. and Leao, V.A., 2007. Bioleaching and chemical leaching as an integrated process in the zinc industry. Minerals Engineering, 20(6): 591-599.

Szekely, J., Evans, J.W. and Sohn, H.Y., 1976. Gas solid reactions. Academic Press, New York, 400 pp.

Terry, B. and Monhemius, A.J., 1983. Acid dissolution of willemite ($(Zn,Mn)_2SiO_4$) and hemimorphite ($Zn_4Si_2O_7(OH)_2H_2O$). Metallurgical Transactions B - Process Metallurgy, 14(3): 335-346.

Umino, S. and Newman, J., 1997. Temperature Dependence of the Diffusion Coefficient of Sulphuric Acid in Water. Journal of the electrochemical society, 144(4): 1302-1307.

Zhou, H.-m., Zheng, S.-l., Zhang, Y. and Yi, D.-q., 2005. A kinetic study of the leaching of a low-grade niobium-tantalum ore by concentrated KOH solution. Hydrometallurgy, 80(3): 170-178.

CAPÍTULO 4

THE EFFECT OF THE IRON CONTENT IN ZINC SILICATE CONCENTRATE LEACHING WITH SULPHURIC ACID.

Abstract

This work shows that the iron content in zinc silicate concentrates does not affect zinc extraction as the dissolution kinetics of concentrates with either high (10-11%) or low iron (3%) content is similar. The activation energy determined for the high-iron concentrate leaching, 13.1 ± 5.1kcal/mol, is statistically similar to that observed for the low-iron material, 16.0 ± 2.2kcal/mol. This suggests that the leaching of both solids presents the same rate-controlling step. The statistical analysis of the leaching experiments showed that increasing the iron content of the silicate from 5% to 9% iron does not result in a significant reduction in extractions, as 98.5% zinc dissolution was achieved for the low-iron concentrate. In the meantime, a zinc extraction of 97.5% was observed for the high-iron sample. Furthermore, a high iron content in the silicate concentrate enables a higher mass recovery during flotation. A flowsheet is proposed utilizing the high iron content in silicate concentrate for impurity removal.

Key words: Leaching, modelling, Reaction Kinetics

4.1. Introduction

The roasting of zinc sulphide concentrates produces zinc, iron and other metal oxides, named as calcine (Çopur *et al.*, 2004). Zinc ferrites are one of the major species in the residues of zinc calcine leaching (Youcai and Stanforth, 2000). These ferrites can be very refractory to chemical attack and one method for zinc recovery from them is to leach these residues with hot and concentrated sulphuric acid solutions, but it will always dissolve a considerable amount of iron. The latter also requires a large quantity of acid during leaching and then a series of downstream iron and unwanted metal removal steps (Youcai and Stanforth, 2000). Several processes to remove dissolved iron have been applied at zinc industries, such as the jarosite [$XFe_3(SO_4)_2(OH)_6$], the goethite (FeOOH) and hematite (Fe_2O_3) processes; each of them having its own advantages and disadvantages (Pappu *et al.*, 2006). Notwithstanding, a small iron concentration in the zinc process is beneficial. Raghavan et al. (1998) has proposed that there are two major steps to remove impurities from the zinc sulphate solution to those levels required for the electrolyte. The first stage takes place in the neutral leaching step where co-precipitation of several deleterious impurities such as antimony, arsenic, germanium, occurs along with that of iron hydroxide (equation 4.1). The second step comprises cementation with zinc dust.

$$2FeSO_4 + 3ZnO + MnO_2 + 2H_2SO_4 + H_2O \rightarrow 2Fe(OH)_3 + 3ZnSO_4 + MnSO_4 \quad (4.1)$$

In the case of silicate concentrates, Souza (2000) has devised an integrated process to treat zinc silicate concentrates in the same plant that processes zinc sulphide concentrates by the RLE process (the integrate process). Among the different options

available, the author has suggested only one step of zinc silicate leaching. In the latter, there is a stepwise addition of sulphuric acid whereby the silicate is dissolved with a minimum silica gel formation. The neutralisation of the residual acidity with lime or limestone to pH 4.0 provides good settling and filtration properties of the leaching residue. This leaching process, in operation at Três Marias zinc facility, presents high zinc recovery (> 98%), treating 350,000 tonnes/year of zinc silicate concentrate (Brook Hunt 2006). Although there is no reference to the iron influence during leaching in the integrated process, the interest for the hydrometallurgical processing of high iron silicate concentrates appeared when the Vazante Mine, in Brazil (the zinc silicate source), noticed the occurrence of high-iron silicate ores that would be submitted to the flotation step, which precedes the hydrometallurgical treatment.

The purpose of the present work, therefore, is to examine the effect of the iron content in concentrates on both zinc dissolution kinetics and recovery. A new concept of treatment is proposed using the iron content in the concentrate to eliminate impurities.

4.2. Materials and Methods

The leaching of zinc silicate flotation concentrates with high and low iron contents was studied. These two different concentrates are referred to as low- and high-iron concentrates throughout the paper.

The chemical analysis of both the high- and low-iron flotation concentrates is presented in table 4.1. The high-iron concentrate contains 35-39% zinc and 7-11% iron, whereas the low-iron sample has more zinc (46%) and less iron (~3%). Prior to the leaching

experiments, these concentrates were dry ground and wet sieved to yield a particle size distribution between 150 and 38 μm. Zinc and iron contents as well as surface area, total porous volume and pore average diameter of the different sieved fractions are also presented in table 4.1.

Table 4.1. Chemical analysis (Zn and Fe) and surface parameters of different screened fractions of both the low- and high-iron zinc silicate concentrates.

		Unit	150-105 μm	105-75 μm	75-53 μm	53-45 μm	45-38 μm	Bulk*
High-iron silicate concentrate	Zn	(%)	39.37	39.66	35.57	35.16	34.06	34.09
	Fe	(%)	7.96	9.76	11.74	10.29	11.09	9.07
	SiO_2	(%)						18.31
	Surface area	m^2/g	1.2	1.0	0.6	0.6	1.0	-
	Total porous volume	mm^3/g	3.6	3.3	2.5	2.5	2.5	-
	Pore average diameter	Nm	12.1	13.1	17.9	18.0	9.8	-
Low-iron silicate concentrate	Zn	(%)	46.92	46.00	46.88	46.58	47.28	42.5
	Fe	(%)	3.74	2.92	3.19	3.02	3.25	4.40
	SiO_2	(%)						22.1
	Surface area	m^2/g	0.8	0.5	0.5	0.5	0.7	-
	Total porous volume	mm^3/g	3.5	1.4	1.3	2.1	1.3	-
	Pore average diameter	nm	17.6	11.6	10.8	15.8	7.4	-

Also 0.01-002%, Cd, 0.002%, Cu, 0.002% Co and 1.02-1.10% Pb.

Chemical leaching experiments were carried out batchwise in a closed waterjacket borosilicate glass reactor with 750 mL total volume and agitation was provided by a magnetic stirrer. That enabled adequate dispersion of the mineral particles without evaporation loss of the solution. The solution volume was 500 mL and the solid concentration 10 g/L. Leaching solutions were prepared using reagent grade chemicals (H_2SO_4, *Synth*) and distilled water. At selected time intervals, a known amount (3 mL)

of slurry was withdrawn and filtered. The zinc extraction was determined by analyzing zinc concentration in solution (Atomic Absorption Spectrometry, Perkin Elmer AAnalyst 100), and for every sample withdrawn from the reactor, the volume change was taken into account for the zinc extraction determinations.

Batch leaching experiments under industrial conditions (150 g/L solids; 70±2 ^{o}C; 7 h retention time; 35 g/L final acid concentration and 2.75 L total volume) were also carried out to determine zinc extraction from three different zinc flotation concentrates, assaying 5%, 9% and 12% iron. These experiments aimed to confirm those results achieved during the kinetic studies (low solid concentrations and pulp volume). In addition, batch leaching experiments were also carried out with both the magnetic and non-magnetic products of a magnetic separation step performed on the flotation concentrate. These leaching experiments were performed at the following experimental conditions: 160g/L initial sulphuric acid concentration, 10% solids, 70-75^{o}C and 7h leaching time for the both the feed and non-magnetic product while the magnetic material was leached in similar conditions expect the temperature (90-95^{o}C) and the leaching time (5 hours).

Table 4.2 – Chemical Analysis of the iron content in the zinc silicate concentrates

Element	Conc. 5% Fe (%)	Conc. 9% Fe (%)	Conc. 10% Fe (%)
Zn	42.56	40.09	39.20
Fe	5.74	9.07	11.75
Pb	1.15	1.02	1.03
SiO_2	21.12	18.31	19.58

Surface area and pore volume were determined by nitrogen adsorption. Nitrogen isotherms were performed with a Nova 1000 High Speed Gas Sorption Analyzer (*Quantachrome*). Sample degassing was carried out at 80^{o}C, for 24 hours, to avoid decomposition. Nitrogen adsorption was performed at -196°C. Data were collected from a relative pressure (p/p_0) of 0.05 to 0.98. A large sample (~4.0g) was used and the Nova 1000 parameters (equilibration tolerance, time to remain in tolerance and maximum equilibration time) were set at 0.05, 360 and 720, respectively, to improve the accuracy of low surface area measurements with nitrogen adsorption.

X-ray diffraction was carried out at on a Shimadzu 600 diffractometer equipped with an iron tube and graphite monocromator. Willemite is the main mineral phase and quartz, hematite and hemimorphite were also present as minor phases in the low-iron concentrate while franklinite and dolomite were also observed in the high-iron concentrate. However, hemimorphite was not present in the latter; therefore zinc in this concentrate is associated with willemite and franklinite (a minor species) (figures 4.1 and 4.2).

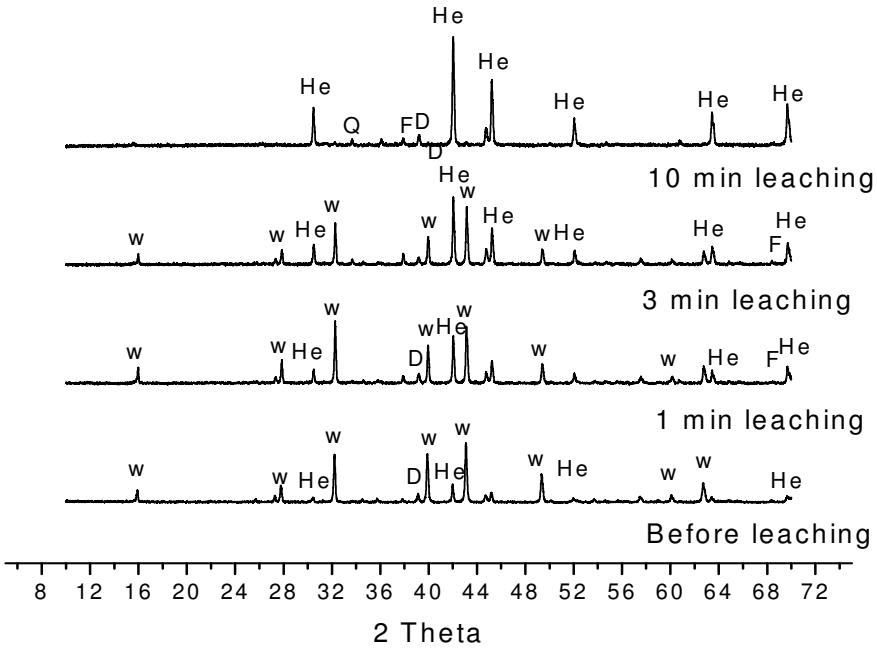

Figure 4.1. XRD pattern of the high-iron zinc silicate concentrate. Q: quartz, He: hematite, w: willemite, F: Franklinite, D: dolomite.

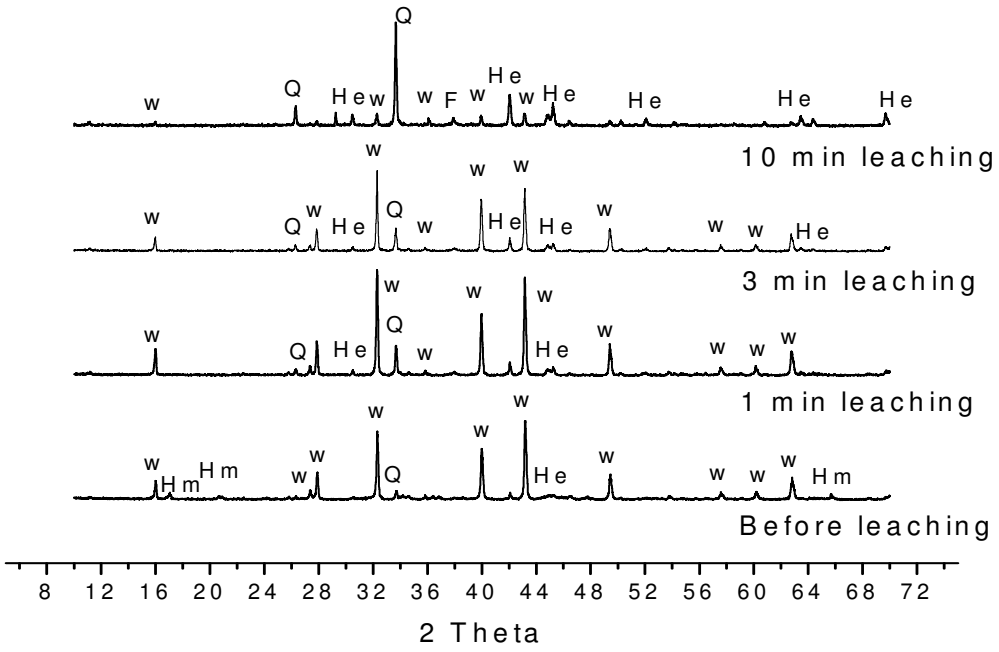

Figure 4.2. XRD pattern of the low-iron zinc silicate concentrate. Q: quartz, He: hematite, w: willemite, F: Franklinite, Hm: Hemimorphite.

The analyses of both concentrates and leaching residues were also carried out by SEM-EDS. The samples were coated with graphite by electro-deposition, using a Jeol JEE 4C instrument and observed in a JEOL JSM 5510 scanning electron microscope (SEM), equipped with a spectrometer for micro-analysis, based on an Energy Dispersive X-ray Spectroscopy System (EDS), and having an accelerating voltage of 0.5-30kV. Electron microprobe analysis have confirmed willemite as the main zinc mineral since the metal content of different grains is similar to that of a pure mineral (theoretical, table 4.2 and figure 4.3). As show in figure 4.3 (b) iron is not present in the willemite structure.

Table 4.3. EDS analysis (Zn, Si and O) of the zinc silicate calcine (average of 6 points).

Element	EDS analysis	Pure willemite
Zn	55.97	58.67
Si	12.56	12.61
O	31.57	28.72

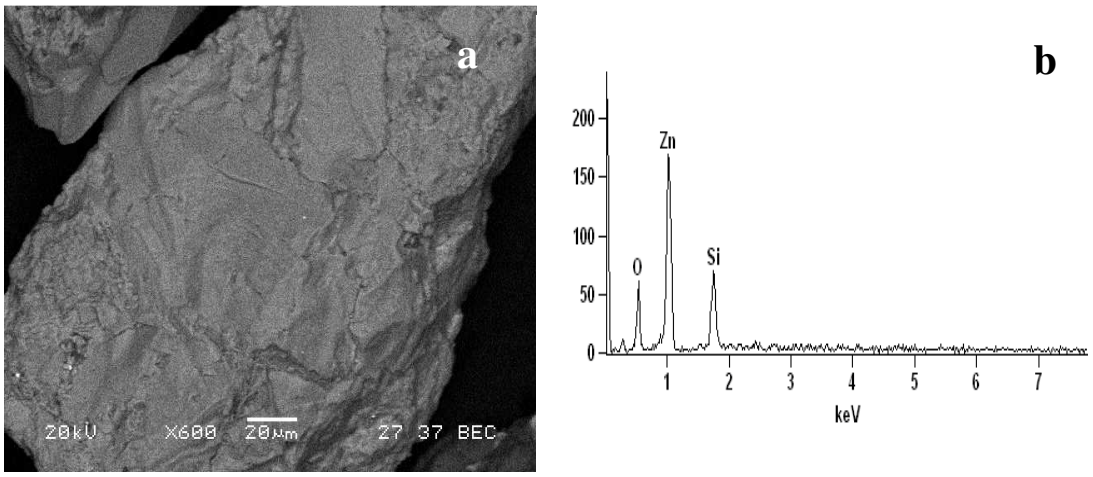

Figure 4.3. Willemite particle (a) and its EDS spectrum (b) showing the presence of oxygen, zinc and silicon as the only elements in the mineral particle.

4.3. Results and discussion

4.3.1. Effect of the agitation speed

The effect of the agitation speed on zinc extraction for the high- and low-iron concentrates were assessed in the range 360-720 rpm. The stirring rate did not affect the zinc extraction regardless of the iron content in both concentrates. Therefore, the dissolution process did not seem to be controlled by mass transfer through the liquid boundary film, despite the possible change in solution viscosity caused by silica gel formation. Unless otherwise stated, the stirring speed was kept at 600 rpm.

4.3.2. Effect of the temperature

Figures 4.4 and 4.5 show zinc extractions as a function of temperature, in the range 30-70ºC, for the high- and low-iron materials, respectively. These results show that zinc extraction is fast, occurring in less than 600s for the high-iron sample and slightly slower for the low-iron concentrate (1200s). Furthermore, temperature has an important influence on the zinc extraction rate, irrespective of the iron content in the concentrate samples. Similar results were observed by Bodas (1996) and Espiari et al. (2006), that carried out leaching experiments with a zinc silicate containing hemimorphite ($Zn_4Si_2O_7(OH)_2.H_2O$) and smithsonite ($ZnCO_3$) as major zinc minerals. Abdel-Aal (2000) also studied the leaching of a zinc silicate ore containing willemite and hemimorphite as major zinc phases and small amounts of smithsonite, and observed that increasing the temperature from 40 to 70ºC improved zinc extraction (from 70% to

95%). Similarly, Souza et al. (2007) also verified the temperature influence on the leaching of a zinc silicate calcine in the range 30-60ºC.

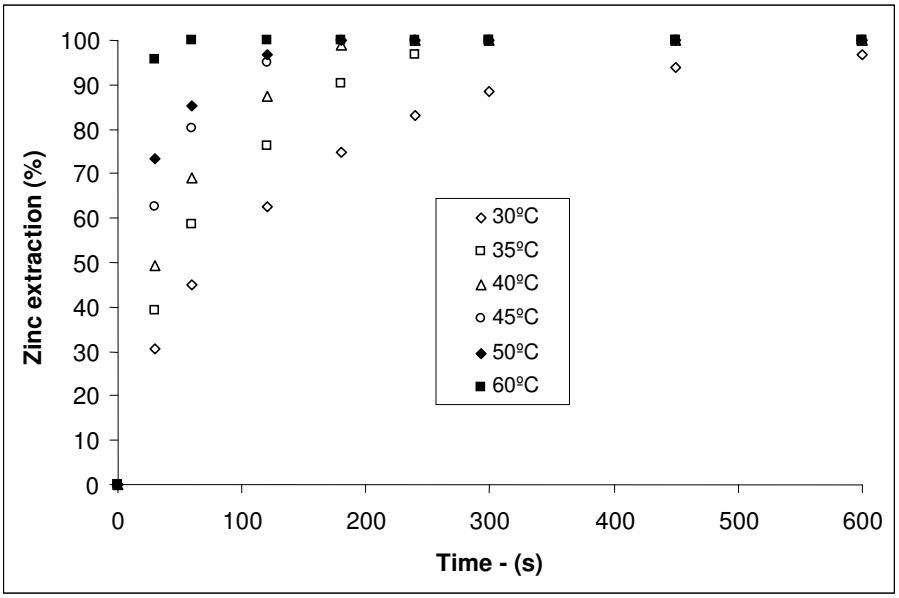

Figure 4.4. Effect of temperature on zinc extraction for the high-iron silicate. 0.4 mol/L H_2SO_4, 10 g/L solids, agitation speed 600 rpm and particle size 75-53 μm.

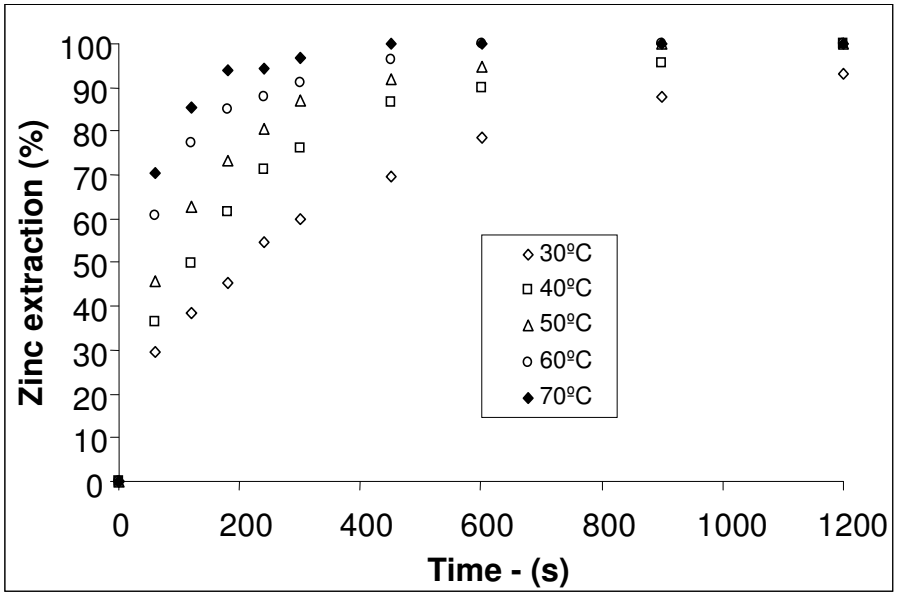

Figure 4.5. Effect of temperature on zinc extraction for the low-iron silicate. 0.4 mol/L H_2SO_4, 10 g/L solids, agitation speed 600 rpm and particle size 75-53 μm.

4.3.3. Effect of acid concentration

Figures 4.6 (high-iron) and 4.7 (low-iron) present the effect of sulphuric acid concentration on zinc extraction as a function of time. Zinc extractions increase gradually with the sulphuric acid concentration in both cases, in the range assessed in this study (0.1 to 1 mol/L H_2SO_4). This behaviour was observed in previous works carried out by Bodas (1996), Abdel-Aal (2000), Espiari et al. (2006) and Souza et al. (2007), in experiments performed in sulphuric acid medium. Terry and Monhemius (1983) also studied the effect of sulphuric, nitric, phosphoric and hydrochloric acid concentrations upon the zinc dissolution from a willemite sample. The authors observed that the zinc dissolution rate was strongly dependent on acid concentration and the acid anion (SO_4^{2-}, PO_4^{3-}, Cl^- and NO_3^-) and suggested that the difference in the reactivity order was a function of the complex affinity for the zinc ion. In spite of the higher leaching rate observed in the hydrochloric acid medium, the present work was carried out with sulphuric acid solutions, since this is the standard reagent in industrial practices.

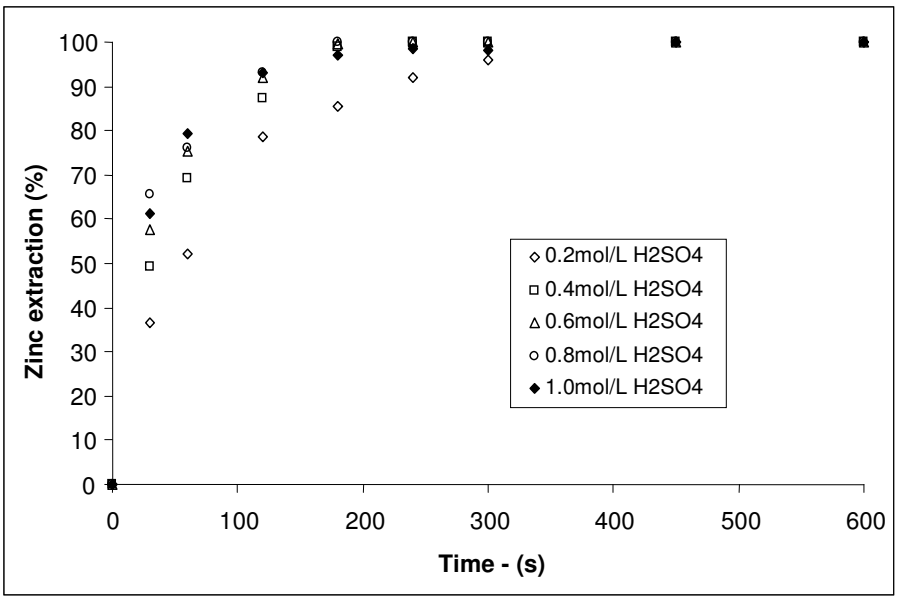

Figure 4.6. Effect of acid concentration on zinc extraction from the high-iron content silicate. Stirring speed 600 rpm, 10 g/L solids, temperature 40 ºC and particle size 75-53 µm.

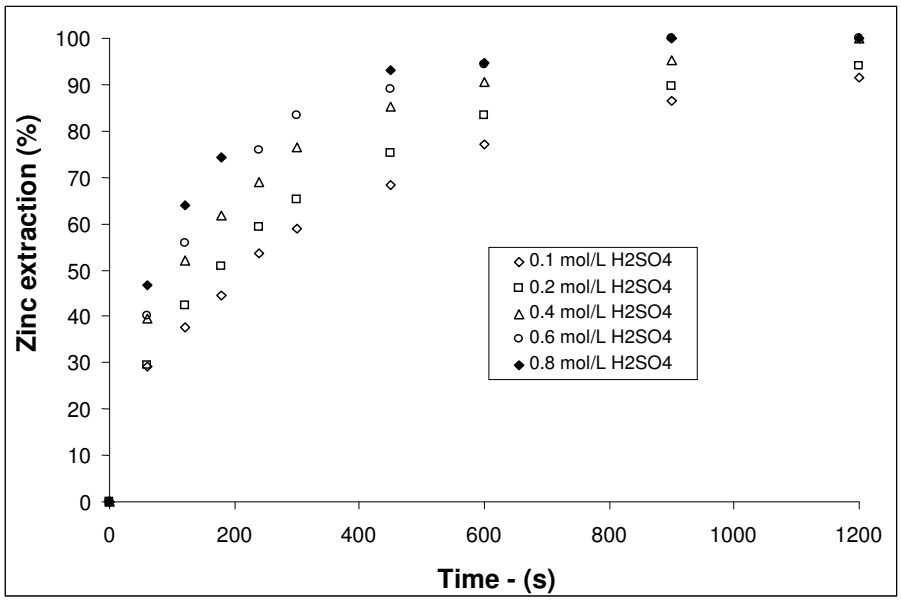

Figure 4.7. Effect of acid concentration on zinc extraction from the low-iron silicate. Stirring speed 600 rpm, 10 g/L solids, temperature 30 ºC and particle size 75-53 µm.

4.3.4. Effect of the particle size

The effect of the particle size upon zinc extraction is presented in figures 4.8 and 4.9 for the high- and low-iron concentrates, respectively. The decrease in particle size enhanced zinc dissolution in the beginning of the experiments, but it can be noticed that such fast leaching reactions are not affected by the particle size since zinc extractions are about the same at the end of the experiment irrespective of the size fraction studied.

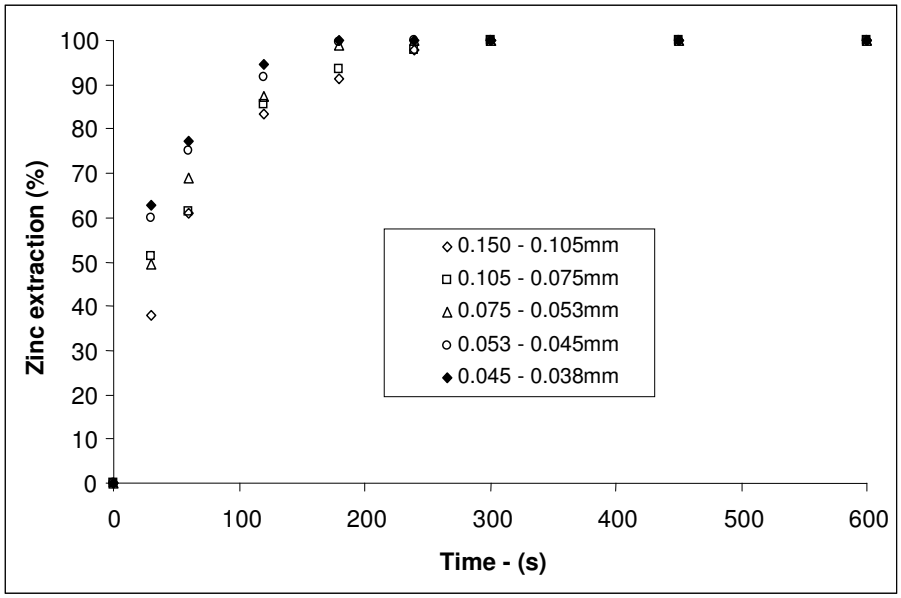

Figure 4.8. Effect of particle size on zinc extraction from the high-iron content silicate. (stirring speed 600 rpm, 10 g/L solids, temperature 40 ºC and 0.4 mol/L H_2SO_4).

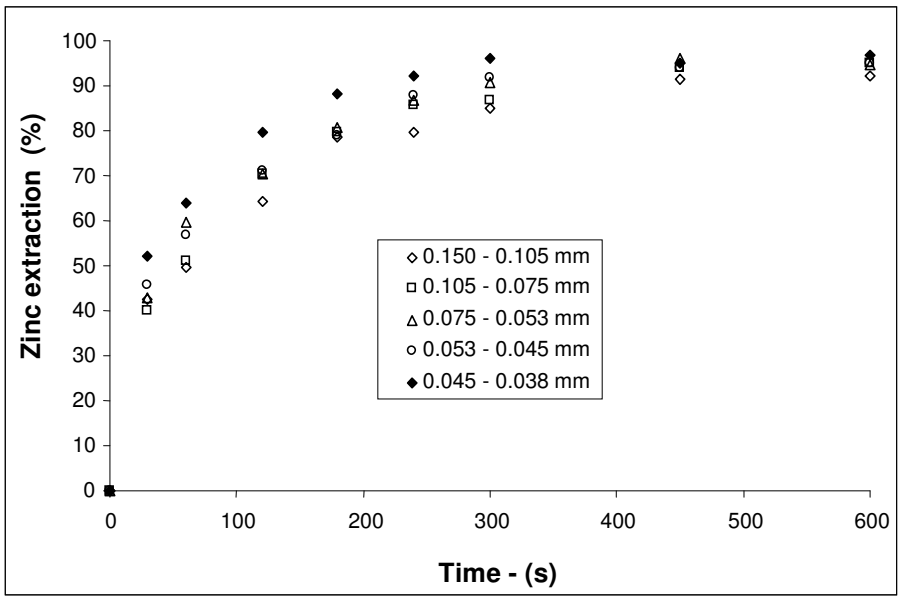

Figure 4.9. Effect of particle size on zinc extraction from the low-iron content silicate. (Stirring speed 600 rpm, 10 g/L solids, temperature 40 ºC and 0.4 mol/L H_2SO_4).

4.3.5. Characterization of the leaching residues

The morphology of both the high- and low-iron zinc silicate flotation concentrates before and after 1, 3, and 10 minutes of leaching was examined by SEM-EDS and presented in figure 4.10, for the zinc-containing phases. The micrographs of the high-iron material are presented in the first column (A) and those of the low-iron, depicted in the second column (B). The solids particles before leaching present a natural rough surface, as observed in figures 4.10 (A.1) and 4.10 (B.1). The leaching residues show a progressive increase in the roughness and porosity, regardless of the iron content in the concentrate (figures 4.10 (A.2) to 4.10 (A.4) and 4.10 (B.2) to 4.10 (B.4)). In spite of the surface degradation generated by the leaching process, the SEM-EDS analysis suggests that the particle surface does not present any reaction product layer. Confirming figures 4.1 and 4.2, willemite progressively disappears while the less

soluble phases predominate at the late stage of leaching (quartz and hematite) (data not shown). Furthermore, as the low-iron concentrate has a slower leaching kinetics, willemite is observed in the 10 min leaching residue (figure 4.2).

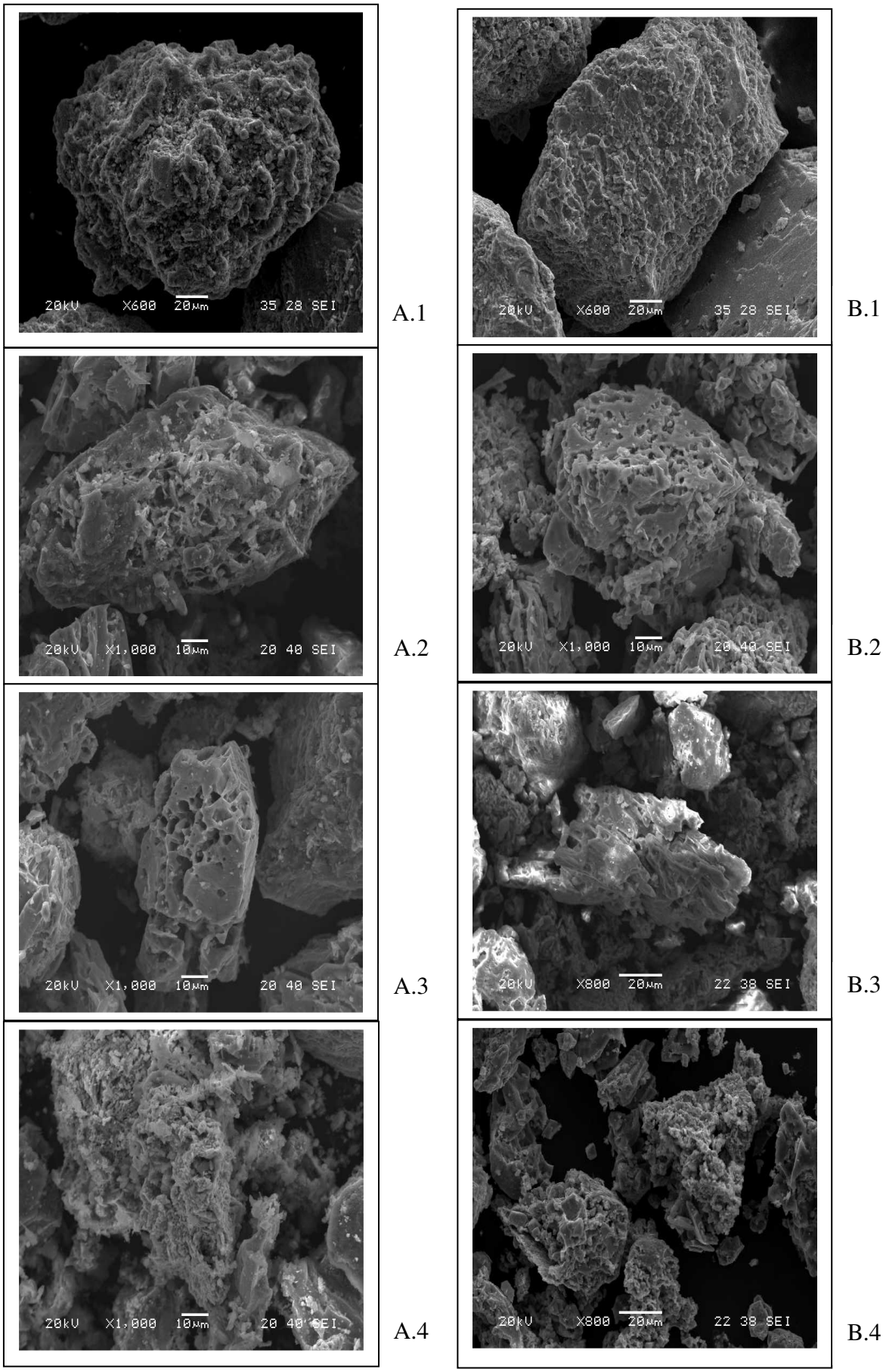

Figure 4.10. Particles of zinc containing phases for the high- (A) and low-iron (B) concentrates. Before leaching (A.1, B.1); after 1min (A.2 and B.2); 3 min (A.3 and B.3) and 10 min (A.4 and B.4).

4.3.6. Kinetics studies

Discussing the application of different kinetics models to the leaching of porous materials, a previous work (Souza et al., 2007) observed that the grain model with pore diffusion control could successfully describe the dissolution kinetics of a zinc silicate concentrate. This model considers that the solid reactant is made up of a large number of individual grains of the same size and form, which are similar to the exterior form of the particle (i.e. a spherical particle is formed by spherical non-porous grains). When the chemical reaction resistance is negligible, as compared to that due to pore diffusion, the reaction occurs in a narrow region and this situation is similar to the shrinking core model with ash layer control, applied to nonporous solids (Szekely et al., 1976). In this condition, the model gives the following expression for spherical particles (Georgiou and Papangelakis, 1998):

$$1-3(1-\alpha)^{\frac{2}{3}}+2(1-\alpha)=k_D t \qquad \text{where} \quad k_D=\frac{3bD_{eff}[H_2SO_4]^n}{r_0^2\rho_{silicate}(1-\varepsilon_0)} \tag{4.2}$$

Also k_D can be written as $k_D = A.k_0.[H_2SO_4]^n$ where A stands for area of reaction; α, the fractional conversion; k_D, for kinetic parameter for product diffusion control; b, for stoichiometric coefficient; $\rho_{silicate}$, for molar density of the silicate; r_0, for particle radius; n order of reaction with respect to sulphuric acid; D_{eff}, for effective diffusion coefficient, k_0 for a Arrhenius temperature dependent constant, $[H_2SO_4]$ for the acid concentration and n for the reaction order.

In the present work, the zinc silicate leaching kinetics (both for the low- and high-iron concentrates) could also be fitted to the grain model with porous diffusion control ($r^2 > 0.98$) at different temperatures. Figures 4.11 presents the Arrhenius plot produced from the rate constants, k_D, at different temperatures. The activation energy determined for the high-iron material is statistically similar to that observed for the low-iron concentrate, 13.0 ± 5.1kcal/mol and 16.0 ± 2.2kcal/mol (95% confidence interval), respectively which corroborates that the leaching of both solids presents the same rate-controlling-step, i.e. diffusion on the particle's pores, as observed by Souza et al. (2007) for a similar zinc concentrate. The latter determined an activation energy value of 12.4 ± 0.7kcal/mol for the dissolution kinetics of a calcined sample of the low-iron zinc silicate, which is analogous to the values observed in this work. Similarly, Terry and Monhemius (1983) found, respectively, 11.77kcal/mol for the dissolution of willemite samples in sulphuric acid solution, and suggested that the process was chemically controlled. The values observed in the present work are likely derived from the parallel nature of diffusion and chemical reaction in porous solids, since the overall reaction rate of the process is always proportional to the reaction rate of the chemical step, irrespective of whether or not the process is chemically controlled (Souza et al., 2007, Sohn and Wadsworth, (1979). This implies that the apparent activation energy is the average of that for intrinsic reaction and diffusion. The reaction order (fig. 4.12), similarly, is also influenced by the parallel nature of the chemical reaction and diffusion, and the values observed for both materials (around 0.55) also suggest that the dissolution of the high- and low-iron concentrates have the same rate-determining step.

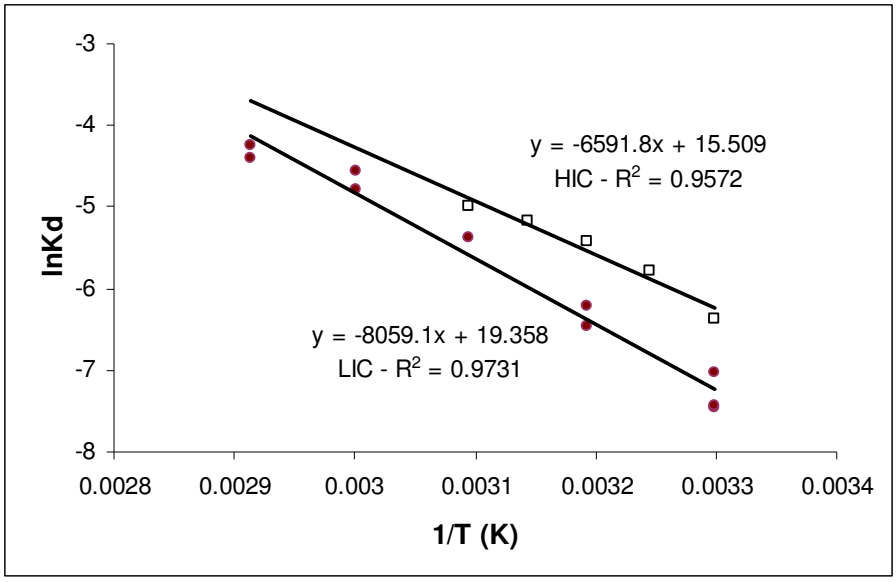

Figure 4.11. Arrhenius plot. Agitation speed 600 rpm, 0.4mol/L H_2SO_4, 10g/L solids (w/v) and particle size 75-53µm.

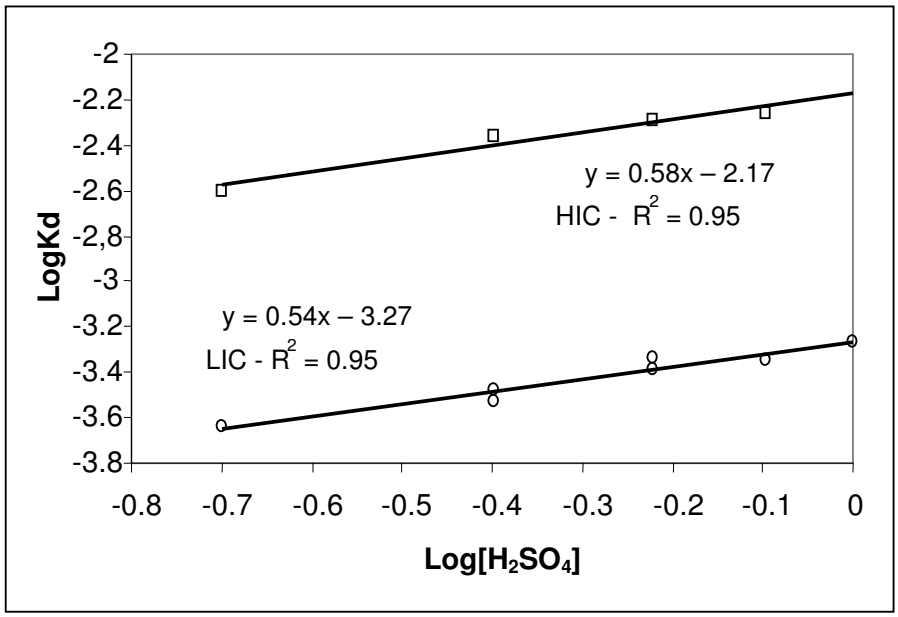

Figure 4.12. Log versus Log plot. Agitation speed 600 rpm, 10g/L solids (w/v), temperature 40ºC to HIC (high iron content), temperature 30ºC to LIC (low iron content) and particle size 75-53µm.

4.3.7. Statistical study of the relevance of iron content in the leaching of the zinc silicate flotation concentrate

Experiments were carried out with three zinc silicate concentrates assaying 5%, 9% and 12% iron so that the effect of iron content in zinc leaching was determined. These experiments were carried out under similar conditions (acid concentration, leaching time, solid content and temperature) to those currently performed at the Três Marias Zinc facilities in Brazil. Table 4.3 presents both zinc and iron extractions as a function of iron content in the zinc concentrate as well as their respective means and standard deviations. High zinc extractions were observed in all experiments, regardless of the iron level in the concentrate (higher than 97% zinc extraction was achieved). The analysis of variance (ANOVA) and the Tukey pairwise comparisons of the average zinc extractions for the 5% and 12% Fe concentrate indicate that the iron content of the concentrate statistically affects the zinc leaching ($f_0 > f_{0.05;\ 2;\ 12}$ or $31.88 > 3.89$ and $P < \alpha$ or $0.000 < 0.05$). Notwithstanding, increasing the iron content from 5% to 9% iron does not result in a statistically significant (different) reduction in zinc extraction. This is because the confidence interval of the difference of the means, achieved from the experiments carried with the 5% and 9% Fe concentrates and based on the Tukey pairwise comparisons, pass through zero. The relevance of these results for the industrial practice will be discussed in details in the next section.

Table 4.4. Zinc and iron extractions as a function of the iron content in the zinc silicate concentrates.

Experiments	Zinc extraction (%)			Iron extraction (%)		
	5% Fe	9% Fe	12% Fe	5% Fe	9% Fe	12% Fe
1	98.5	98.5	98.4	13.1	31.2	-
2	99.0	99.0	98.7	31.3	36.2	19.7
3	98.9	98.9	98.9	24.1	15.0	11.2
4	98.7	98.7	98.6	16.2	17.7	14.5
5	98.7	98.7	98.4	20.7	-	17.8
Mean	98.7	98.7	98.6	21.1	25.2	15.8
Standard Deviation	0.22	0.22	0.20	7.1	10.4	3.7

4.3.8. Industrial implications of the iron content in the silicate concentrates

4.3.8.1 Treatment of flotation concentrates with integration with the RLE process

Low iron content is a drawback for the processing of zinc silicate concentrates as iron plays an important role during the removal of impurities such as arsenic, germanium and antimony (Raghavan *et al.*, 1998). The integrated technology to treat zinc silicate concentrates along with zinc sulphide calcines (Souza, 2000) applied at the Três Marias facility, uses the concept of impurities removal by adsorption in ferric iron during the neutral leaching of calcines (ZnO) produced from zinc sulphide roasting. This is achieved as the pregnant solution, produced during the silicate leaching, is sent to the calcine treatment step, where the high pH (4-4.5) causes iron precipitation along with

impurity removal. This approach is cost-effective in the zinc industry (Brook-Hunt, 2005).

It is well known that a series of strong acid leaching steps are required to achieve high zinc recoveries from sulphide concentrates with high-iron content due to the formation of zinc ferrites during roasting of such sulphides (Brook-Hunt, 2005). As the silicate also contains a natural form of zinc ferrites (franklinite), the same behaviour would be expected for zinc silicate flotation concentrates when the iron level is increased. Nevertheless, it is shown in the present work, through the kinetics study of high- and low-iron flotation concentrates, that the leaching of both materials is similar. This is an important finding for zinc silicate facilities, because the specification of the raw-material could be less restrictive, so that high-iron concentrates could be processed (up to 12%). The present work appoints that concentrates with less than 9% iron did not reduce zinc recovery as compared to those with 5% iron. Noticeable was that even with 12% iron, zinc recoveries higher than 97.5% were accomplished. Therefore, the leaching step needs not to be changed on moving from a sulphide treating plant to a silicate processing facility or when the iron content in the flotation concentrate increases with time. This contributes to double savings. Firstly, the capex (capital expenditure) associated with the treatment of high-iron concentrates is low because the route would not be changed. Secondly, the Opex (operating and maintenance expenditure) is also reduced as concentrates with high iron content are always cheaper.

Furthermore, when the iron content in the concentrate is increased (zinc content is reduced), the overall zinc recovery in the flotation step is improved, as shown in figure 4.13 for pilot-plant flotation experiments carried out with these zinc silicates. In those zinc leaching facilities integrated with ore concentration plants, such as Votorantim Metais in Brazil, the overall zinc recovery could be increased significantly, more than 8%, when it is possible to increase the iron content in the flotation concentrate.

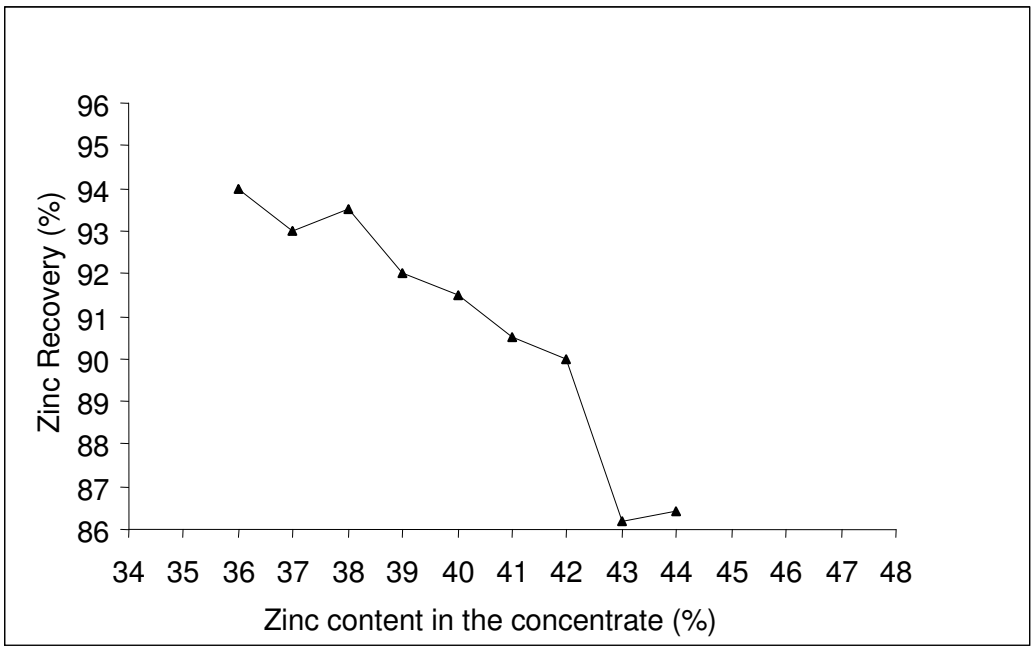

Figure 4.13. Zinc mass recovery for different zinc content in the concentrate.

4.3.8.2. Treatment of silicate concentrates without integration with the RLE process.

For those plants treating only zinc silicate concentrates, a different concept can be proposed using the iron content in the zinc silicate concentrate itself to remove impurities. The simplified flowsheet of this new concept is showed in figure 4.14 which introduces a magnetic separation step performed on the flotation concentrate and produces two different phases. The first one has a low-iron content (~6%) that accounts for 90% mass recovery (non-magnetic concentrate) (table 4.4), which is leached at mild

conditions where iron dissolution is not an issue. A second fraction, with high-iron content (~19%) (magnetic concentrate), requires stronger leaching conditions (table 4.5) so that iron is dissolved and precipitated afterwards when the pH is increased, removing the impurities.

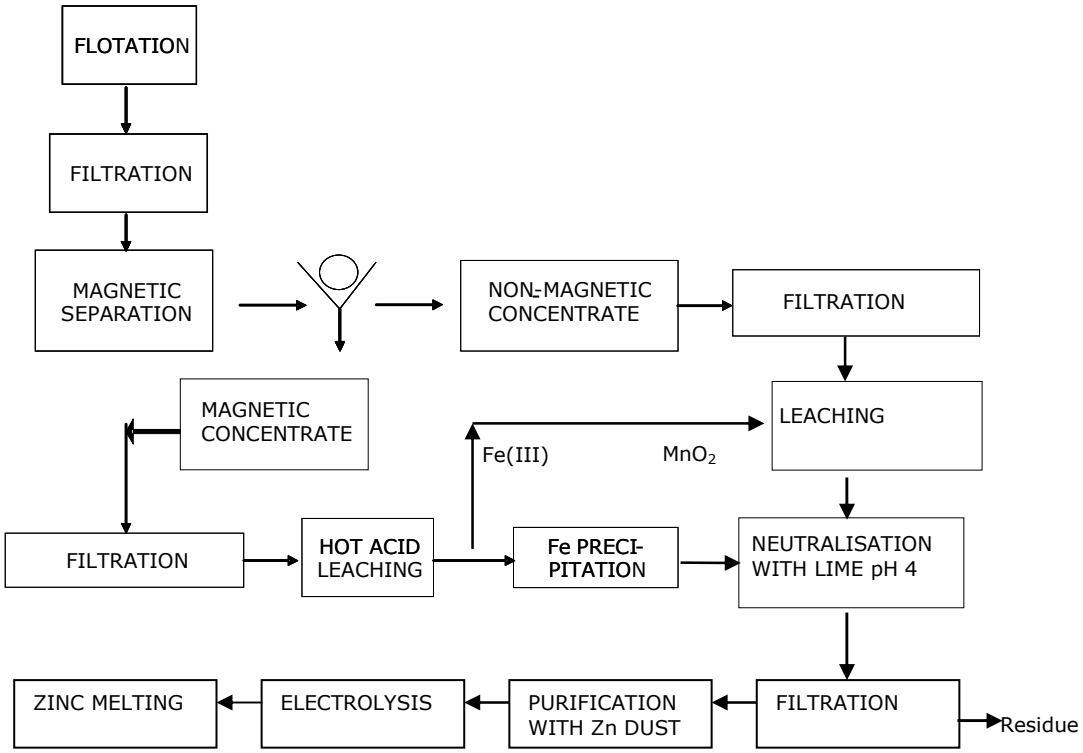

Figure 4.14. New concept to treat flotation/magnetic silicate concentrate with high-iron content.

Table 4.5. Zinc concentrate achieved during the magnetic separation step.

Material	Ratio (%)	Moisture (%)	Zn (%)	Fe (%)	SiO_2 (%)
Flotation Concentrate	-	13.10	38.48	8.95	21.58
Non-magnetic Concentrate	90	13.60	39.89	6.21	23.11
Magnetic Concentrate	10	8.20	26.86	19.13	16.88

Table 4.6. Zinc recoveries in the leaching experiments with the zinc silicate concentrate and both magnetic and non-magnetic materials.

Parameters	Flotation concentrate	Non-magnetic concentrate	Magnetic concentrate
Zinc concentrate			
Moisture (%)	13.10	13.60	8.20
Zn (%)	38.48	39.89	26.86
Fe (%)	8.95	6.21	19.13
SiO_2 (%)	21.58	23.11	16.88
Pregnant leach solution			
Zinc (g/L)	109.40	135.80	104.50
Fe_{total} (g/L)	1.84	1.61	8.85
Fe^{2+} (g/L)	1.23	1.12	2.01
Fe^{3+} (g/L)	0.61	0.49	6.84
Final acidity (g/L)	35-40	35-40	70-80
Residues from the concentrate leaching			
Insoluble Zn (%)	1.74	1.69	0.58
SiO_2 (%)	46.48	53.94	26.05
Overall zinc recovery (%)	97.90	98.18	98.60

Leaching conditions: for flotation and non-magnetic concentrates: temperature 70-75^{o}C, pulp density 10%, retention time 7h. For magnetic concentrate: temperature 90-95^{o}C, pulp density 10%, retention time 5h.

Leaching of the magnetic and non-magnetic concentrates produced high zinc recoveries, similarly to the flotation concentrate, as presented in table 4.6. This demonstrates that the proposed conditions for leaching are satisfactory and can be applied on an industrial

scale as high iron concentration was observed in the pregnant leach solution (magnetic concentrate). According to table 4.6, it can be seen that zinc recoveries are high (>98%), with the advantage that it is possible to produce a source of ferric iron (more than 6 g/L), sufficient for trace impurity removal.

Several advantages can be foreseen in the proposed flowsheet. Firstly, the existing industrial facilities can be utilized to leach the non-magnetic concentrate because leaching can be carried out in mild conditions. A consequence of this is that concentrates with higher iron content could be processed without affecting zinc recovery, therefore dirtier concentrates could also be treated. Another advantage is that iron dissolution from the magnetic concentrate acts as a source of soluble iron for impurities removal in the purification step. This eliminates the necessity of the use of sulphide concentrates in the same process, i.e., the efficient treatment of 100% silicate concentrate becomes feasible.

4.4. Conclusions

The leaching of zinc silicate concentrates with high- and low-iron content was studied. Zinc extraction increased gradually with sulphuric acid concentration for both materials, in the range of acid concentration assessed in this study (0.1 to 1 mol/L H_2SO_4). The activation energy for the high-iron concentrate (13.1 ± 5.1kcal/mol) leaching was statistically similar to that observed for the low-iron material (16.0 ± 2.2kcal/mol), which suggests that the leaching of both solids presents the same rate-controlling step. The statistical analysis of the leaching experiments shows that increasing the iron content of the silicate from 5% to 9% does not result in a significant (different)

reduction in zinc extraction. This finding has an important industrial application, i.e., the raw materials specification could be less rigorous, enabling more impure concentrates, in terms of iron content, to be treated in the hydrometallurgical plant. In addition, the overall zinc recovery could be increased significantly, more than 8%, by raising the iron content in the flotation concentrate. Also, the leaching step needs not to be changed on moving from a sulphide treating plant to a high-iron silicate processing facility. The proposed flowsheet to treat high-iron silicate concentrates produces appreciable zinc recoveries in the leaching step (above 97.5%).

4.5. Acknowledgments

This work was supported by Votorantim Metais Zinc, "FINANCIADORA DE ESTUDOS E PROJETOS – FINEP", and Universidade Federal de Ouro Preto-UFOP. The CAPES scholarship to P. S. Pina and the assistance of Mr. J. A. Magalhães and Ms. H. K. Reis are gratefully acknowledged.

4.6. References

Abdel-Aal, E.A., 2000. Kinetics of sulfuric acid leaching of low-grade zinc silicate ore. Hydrometallurgy, 55(3): 247-254.

Bodas, M.G., 1996. Hydrometallurgical treatment of zinc silicate ore from Thailand. Hydrometallurgy, 40(1-2): 37-49.

Brook-Hunt, 2005. Minining and metal consultants, "Zinc Smelter study". In: B.H.a.A. Ltd. (Editor). Brook Hunt.

Çopur, M., Özmetin, C., Özmetin, E. and Kocakerim, M.M., 2004. Optimization study of the leaching of roasted zinc sulphide concentrate with sulphuric acid solutions. Chemical Engineering and Processing, 43(8): 1007-1014.

Espiari, S., Rashchi, F. and Sadrnezhad, S.K., 2006. Hydrometallurgical treatment of tailings with high zinc content. Hydrometallurgy, 82(1-2): 54-62.

Georgiou, D. and Papangelakis, V.G., 1998. Sulphuric acid pressure leaching of a limonitic laterite: chemistry and kinetics. Hydrometallurgy, 49(1-2): 23-46.

Pappu, A., Saxena, M. and Asolekar, S.R., 2006. Jarosite characteristics and its utilisation potentials. Science of the Total Environment, The, 359(1): 232-243.

Raghavan, R., Mohanan, P.K. and Patnaik, S.C., 1998. Innovative processing technique to produce zinc concentrate from zinc leach residue with simultaneous recovery of lead. Hydrometallurgy, 48(2): 225-237.

Sohn, H.Y. and Wadsworth, M.E., 1979. Rate processes of extractive metallurgy. Plenum Press, New York, 472 pp.

Souza, A.D., 2000. Integration process of the treatment of concentrates or zinc silicates ore and roasted concentrate of zinc sulphides, WO 0046412.

Souza, A.D., Pina, P.S., Lima, E.V.O., Silva, C.A. and Leao, V.A., 2007. A kinetic study of the sulphuric acid leaching of a zinc silicate calcine. Hydrometallurgy. DOI: 10.1016/j.hydromet.2007.08.005

Szekely, J., Evans, J.W. and Sohn, H.Y., 1976. Gas solid reactions. Academic Press, New York, 400 pp.

Terry, B. and Monhemius, A.J., 1983. Acid dissolution of willemite ($(Zn,Mn)_2SiO_4$) and hemimorphite ($Zn_4Si_2O_7(OH)_2H_2O$). Metallurgical Transactions B - Process Metallurgy, 14(3): 335-346.

Youcai, Z. and Stanforth, R., 2000. Extraction of Zinc from Zinc Ferrites by Fusion with Caustic Soda. Minerals Engineering, 13(13): 1417-1421.

CAPÍTULO 5

CONSIDERAÇÕES FINAIS

Os trabalhos realizados com concentrados de zinco, sulfetos ou silicatos, trouxeram informações relevantes referentes à cinética de dissolução destes concentrados, uma vez que dados sobre a velocidade de dissolução destes sólidos, bem como a energia de ativação e ordem de reação com respeito aos reagentes, podem ser efetivamente empregadas para otimizar o dimensionamento de sistemas industriais.

No estudo da cinética de dissolução da esfalerita com sulfato férrico, verificou-se que modelo de núcleo não reagido pode ser aplicado para descrever o processo. Este era controlado por reação química em sua parte inicial (até 40% de extração) e por difusão no estágio final. Esta mudança no controle foi confirmada por análises de MEV- EDS e também através dos valores de energia de ativação. Na fase inicial do processo de dissolução, a energia de ativação era mais elevada, 6.59kcal/mol (27.54kJ/mol), sugerindo que o processo é controlado quimicamente. No estágio final, a energia de ativação mais baixa, (4.68kcal/mol ou 19.56kJ/mol) é típica de processos controlados por difusão.

A diminuição do tamanho de partícula, apesar de elevar a dissolução do zinco, teve papel secundário no processo de lixiviação. Uma explicação para tal fato seria a porosidade, que aumentava a área superficial do sólido, mesmo para as partículas mais grosseiras.

Para o caso do concentrado de silicato calcinado, os resultados mostraram que a elevação da temperatura e acidez afetavam diretamente a velocidade de lixiviação. Observou-se que, enquanto a lixiviação do calcinado ocorria, havia uma progressiva dissolução da willemita, mantendo-se as fases de quartzo e ferro praticamente inertes. Devido às características físicas do concentrado, o modelo do grão com controle por difusão nos poros pode ser utilizado descrever o comportamento cinético. A energia de ativação, determinada como 50,7 kJ/mol, seria conseqüência da natureza paralela dos processos de difusão e reação química nos poros do sólidos.

Por fim, o teor de ferro em concentrados de zinco é determinante para a avaliação dos rendimentos de recuperação do metal. O estudo do efeito do conteúdo de ferro na lixiviação do concentrado de silicato demonstrou que o aumento de teor até 9% não diminuiu a recuperação do zinco. A descoberta leva a uma importante implicação industrial: a de que pode-se admitir a alimentação de concentrados com teores de ferro mais elevados e de menor preço durante o processamento de minérios silicatados de zinco.

CAPÍTULO 6

CONTRIBUIÇÕES AO CONHECIMENTO

Muito pouco há publicado sobre estudos cinéticos de lixiviação de concentrados silicatados de zinco, particularmente para aqueles da América do Sul, o que confere o caráter inovador dos trabalhos aqui desenvolvidos. Por outro lado, a utilização de modelos cinéticos para sólidos porosos, com ênfase no modelo do grão, é pouco aplicada aos concentrados silicatados. A partir da utilização deste modelo, foi possível determinar a possível etapa controladora do processo (controle por difusão nos poros) de lixiviação ácida do calcinado, bem como, calcular a energia de ativação e a ordem de reação com respeito à concentração de ácido sulfúrico, que são parâmetros importantes no estudo da cinética de dissolução de sólidos em processos hidrometalúrgicos.

Os resultados obtidos no estudo cinético da lixiviação do concentrado silicatados de zinco com alto teor de ferro demonstraram que, diferentemente dos processos usuais de tratamento de concentrados sulfetados, não haveria necessidade de etapas de lixiviação ácida a quente para recuperar o zinco, como ocorre no processo RLE, para obtenção de elevada recuperação (acima de 95%). O estudo ainda propôs uma nova rota comercial para tratamento de concentrado de silicato de zinco com alto teor de ferro (até 9%), utilizando a solubilização deste elemento, seguida de sua precipitação, para a remoção de impurezas (As, Ge, Sb), eliminando a necessidade de integração com processo RLE. Isto conduziu ao estabelecimento de uma rota para tratamento exclusivo de concentrado silicatado.

O estudo também discutiu a possibilidade de se alimentar as usinas de zinco com materiais menos nobres, tendo como conseqüência um aumento correspondente na recuperação de zinco na etapa anterior, a de flotação do minério. A inovação proporciona diversas conseqüências positivas para o processamento de concentrados de silicato de zinco.

As publicações geradas a partir desta tese são descritas a seguir:

- "The leaching kinetics of a zinc sulphide concentrate in acid ferric sulphate", Hydrometallurgy, vol. 89, nº 1-2, pp. 72-81.
- "Kinetics of sulphuric acid leaching of a zinc silicate calcine", Hydrometallurgy, vol. 89, nº 3-4, pp 337-345.
- "The effect of the iron content in zinc silicate concentrate leaching with sulphuric acid". Aceito para publicação no periódico Hydrometallurgy. Doi: 10.1016/j.hydromet.2008.05.049.

CAPÍTULO 7

SUGESTÕES DE TRABALHOS FUTUROS

Diante dos resultados obtidos no presente trabalho e desafios encontrados durante o período de sua elaboração, são sugeridos alguns temas relevantes que poderiam ser estudados em um futuro próximo, relacionados à lixiviação de concentrados ou minérios:

(i) Aplicação do modelo do grão para descrever a cinética de lixiviação de outros sólidos porosos, que não sejam necessariamente fontes de zinco, em outros tipos de meio lixiviante, devido ao sucesso obtido no presente trabalho.

(ii) Estudar a cinética de lixiviação dos concentrados silicatos de zinco, com alto e baixo teor de ferro, em meio alcalino.

(iii) Estudar a cinética de lixiviação dos concentrados silicatos de zinco em presença de outros ácidos inorgânicos e até mesmo orgânicos.

(iv) Estudar a lixiviação dos resíduos de flotação do silicato de zinco em presença de NaOH e H_2SO_4.

(v) Propor e empregar um modelo matemático, baseado no modelo do núcleo não reagido, que possa ser utilizado para descrever a cinética de processos com controle misto e com ordem de reação diferente de 1.

(vi) Utilizar espectroscopia RAMAM para estudar detalhadamente a formação da camada de enxofre elementar durante a dissolução da esfalerita e caracterizar os compostos reduzidos de enxofre possivelmente formados neste processo.